

# Partial Identification of Structural Vector Autoregressions with Non-Centred Stochastic Volatility

Helmut Lutkepohl<sup>a</sup>, Fei Shang<sup>b</sup>, Luis Uzeda<sup>c,\*</sup>, Tomasz Woźniak<sup>d,\*\*</sup>

<sup>a</sup>Freie Universität Berlin & DIW Berlin, Freie Universität Berlin, Boltzmannstr. 20, 14195 Berlin, Germany

<sup>b</sup>Guangdong University of Foreign Studies, Xiaoguzwei, Panyu District, Guangzhou 510006, China

<sup>c</sup>Bank of Canada, 234 Wellington St. W, Ottawa, ON K1A 0G9

<sup>d</sup>University of Melbourne, 111 Barry St., 3053 Carlton, VIC, Australia

---

## Abstract

We consider structural vector autoregressions that are identified through stochastic volatility under Bayesian estimation. Three contributions emerge from our exercise. First, we show that a non-centred parameterization of stochastic volatility yields a marginal prior for the conditional variances of structural shocks that is centred on homoskedasticity, with strong shrinkage and heavy tails—unlike the common centred parameterization. This feature makes it well suited for assessing partial identification of any shock of interest. Second, Monte Carlo experiments on small and large systems indicate that the non-centred setup estimates structural parameters more precisely and normalizes conditional variances efficiently. Third, revisiting prominent fiscal structural vector autoregressions, we show how the non-centred approach identifies tax shocks that are consistent with estimates reported in the literature.

*Keywords:* identification through heteroskedasticity, stochastic volatility, non-centred parameterization, shrinkage prior, normal product distribution

*JEL classification:* C11, C12, C32, E62

---

---

\*The views expressed in this paper are those of the authors and do not necessarily reflect the position of the Bank of Canada.

\*\*Corresponding author. *Email address:* [tomasz.wozniak@unimelb.edu.au](mailto:tomasz.wozniak@unimelb.edu.au).

## 1. Introduction

This paper examines the partial identification of a structural shock in structural vector autoregression models with stochastic volatility (SVAR-SV). Following [Rubio-Ramírez, Waggoner, and Zha \(2010\)](#), we define partial identification of a structural shock as the case in which the parameters of its associated equation within the system are globally identified, up to a sign normalization as in [Waggoner and Zha \(2003b\)](#). Partial identification is particularly important in empirical SVAR applications, where attention often centers on a subset of shocks rather than the full set, or in cases where identification of all shocks is not attainable (e.g. [Lütkepohl and Milunovich, 2016](#)). Common examples include efforts to identify monetary or fiscal policy shocks (see, e.g., [Blanchard and Perotti, 2002](#); [Romer and Romer, 2004](#); [Mertens and Ravn, 2014](#); [Lewis, 2021](#)).

Stochastic volatility, in turn, has become a widely adopted feature in structural models. It is commonly used to improve forecast performance (see, e.g., [Stock and Watson, 2007](#); [Clark, 2011](#); [Clark and Ravazzolo, 2015](#); [Uzeda, 2022](#)) and to study the time-varying nature of economic shocks (see, e.g., [Primiceri, 2005](#); [Cogley and Sargent, 2005](#); [Baumeister and Peersman, 2013](#)). Despite its widespread use, stochastic volatility has not been extensively explored as a source of identification via heteroskedasticity in the spirit of the seminal contribution by [Rigobon \(2003\)](#) with a notable exception being the recent study by [Bertsche and Braun \(2022\)](#).<sup>1</sup>

This paper contributes to fill this gap by combining stochastic volatility modeling with the partial identification of specific structural shocks of interest. To this end, we adopt a *non-centred* parameterization for stochastic volatility models (see, e.g., [Kastner and Frühwirth-Schnatter, 2014](#); [Chan, 2018](#)). This approach differs from the standard *centred* parameterization, which is widely used in various types of applied work with

---

<sup>1</sup>We expand on the distinctions between our approach and theirs later. Also, to be clear, by stochastic volatility we refer to modeling time-varying volatility as a latent process in a state-space framework, noting that identification through heteroskedasticity has also been studied under alternative volatility specifications.

SVAR-SVs. In our setup, the *non-centred* parameterization rewrites the law of motion for the log-volatility of each structural shock in a way that decouples this state variable from the scale parameters (i.e., the standard deviation of the innovations driving the log-volatilities). Similar transformations have been shown to improve computational efficiency in various classes of state-space models (see, e.g., [Frühwirth-Schnatter and Wagner, 2010](#)). However, to date, no study has examined the benefits—or drawbacks—of this parameterization for identification through heteroskedasticity in SVAR-SV models.

In this sense, the paper makes three main contributions. First, we present new theoretical results on the identification of structural shocks through heteroskedasticity in Bayesian-estimated SVAR-SVs. Specifically, we formally characterize how the marginal prior on the conditional variances of structural shocks behaves under the non-centred parameterization and contrast it with the centred case. The key finding is that, compared to the centred specification, the non-centred approach yields a marginal prior centred at homoskedasticity, with strong shrinkage toward it and heavy tails. This setup ensures normalization of conditional variances around value 1, rendering precise estimates of the structural parameters. As an ancillary result to our main theoretical contribution, we also note that, under the non-centred setup, the conditions for partial identification can be verified in practice. We further outline how the Savage–Dickey density ratio (SDDR) can be used to test whether a shock of interest can be identified through stochastic volatility, and describe the conditions under which this approach is valid.

Our second contribution is computational. We conduct a comprehensive Monte Carlo exercise to evaluate the performance of the proposed shrinkage prior in non-centred stochastic volatility models relative to their centred counterparts, across both small and large systems. The results show that parameters crucial for identifying structural shocks—namely, the conditional variances of shocks and the relevant rows of the impact matrix—are estimated more precisely under the non-centred parameterization.

Because the above-discussed theoretical and computational considerations suggest potential implications for practical settings, our third contribution is empirical.

Specifically, we revisit several well-known fiscal-policy SVARs from the literature (see [Blanchard and Perotti, 2002](#); [Mertens and Ravn, 2014](#); [Lewis, 2021](#)) to show that our framework can identify tax shocks through heteroskedasticity, yielding estimates that align closely with those reported in previous studies. Our empirical assessment relies on a Gibbs sampler using advanced techniques: the structural matrix sampler ([Waggoner and Zha, 2003a](#)), row-by-row autoregressive slope sampling ([Chan, Koop, and Yu, 2024](#)), the auxiliary mixture method ([Omori, Chib, Shephard, and Nakajima, 2007](#)), and ancillarity-sufficiency interweaving ([Kastner and Frühwirth-Schnatter, 2014](#)), enabling efficient simulation smoothing under uncertain heteroskedasticity. All procedures are implemented in C++ via the R package `bsvars` ([Woźniak, 2024, 2025](#)), yielding substantial speedups.

A comment is in order regarding our first contribution. Given the substantial evidence of time-varying volatility in macroeconomic and financial variables, the fact that the marginal prior from the non-centred parameterization is centred at, and shrinks toward, a homoskedastic shock may seem counterintuitive. The key nuance is that a *structural shock* can be homoskedastic even when every *variable* in a SVAR is heteroskedastic (see [Lütkepohl and Milunovich, 2016](#)). This is because the conditional variance of the variables in a SVAR can be represented in terms of the conditional variance of the reduced-form VAR residuals, which are convolutions of the structural shocks. For example, if a given structural shock appears in the reduced-form residuals of all VAR equations, it can occur that only this single shock exhibits time-varying volatility, while inducing every variable in the system to be heteroskedastic. Thus, a prior centred at, and shrinking towards, homoskedasticity with heavy tails does not contradict pervasive heteroskedasticity in the data; rather, it reflects that a small number of shocks can drive most of the observed volatility across variables. This interpretation aligns with evidence of comovement in volatility in economic and financial time series documented in factor model-based studies (e.g., [Engel and Kozicki, 1992](#); [Carriero, Clark, and Marcellino, 2016](#); [Castelnuovo, Tuzcuoglu, and Uzeda, 2025](#)).

Perhaps the paper closest to ours is [Bertsche and Braun \(2022\)](#). However, our

approach departs from theirs in several important ways. First, unlike them, we adopt a Bayesian inferential framework, arguably the predominant approach for estimating SVAR-SVs in empirical work. Second, this inferential setup enables us to explore theoretical considerations regarding the marginal prior for the conditional variances that emerge under different stochastic-volatility parameterizations. Third, we address issues of scalability—particularly estimation accuracy—when implementing the proposed identification scheme in larger systems, an exercise that, to the best of our knowledge, is undertaken here for the first time. Our paper also contributes to the growing literature on identification through heteroskedasticity using alternative models and techniques: [Lütkepohl and Milunovich \(2016\)](#) test for a heteroskedastic rank based on the number of independent heteroskedastic processes in a GARCH framework; [Lanne and Luoto \(2021\)](#) propose moment-based tests exploiting kurtosis properties of the structural shocks; [Lewis \(2021\)](#) introduces a non-parametric approach and tests based on autocorrelations of squared residuals under the assumption of non-proportional changes in structural volatilities; [Lütkepohl, Meitz, Netšunajev, and Saikkonen \(2021\)](#) examine testing procedures for two-regime models when the timing of volatility changes is known; and [Lütkepohl and Woźniak \(2020\)](#) develop an SDDR-based identification test using regime-switching heteroskedasticity.

The remainder of the paper is organized as follows. Section 2 discusses heteroskedastic SVARs and presents the two stochastic volatility parameterizations considered. Section 3 characterizes the marginal prior for the conditional variances implied by these parameterizations. Section 4 outlines the conditions for applying the SDDR-based identification test in our framework. Section 5 presents two Monte Carlo studies to assess the estimation accuracy of the non-centred approach. Section 6 reports our empirical results. Section 7 concludes. A complementary theorem and its proof is stated in the Appendix, whereas technical details and additional results are given in the Supplementary Materials.

### Notation

The following notation applies to the main text and technical appendix:  $\mathbf{y}$  denotes the available data,  $\mathbf{I}_N$  is the identity matrix of order  $N$ ,  $\mathbf{0}_{N \times N}$  and  $\mathbf{1}_N$  are a matrix of zeros and a vector of ones of the indicated dimensions, respectively, the operator  $\text{diag}(\cdot)$  puts the vector provided as its argument on the main diagonal of a diagonal matrix, the indicator function  $\mathcal{I}(\cdot)$  takes the value of 1 if the condition provided as the argument holds and 0 otherwise,  $\otimes$  denotes the Kronecker product of matrices.  $A \setminus B$  defines the set with all elements of the set  $A$  that are not in the set  $B$ .  $\Gamma(\cdot)$  denotes the gamma function, and  $K_n(\cdot)$  denotes the modified Bessel function of the second kind. The following notation is used for statistical distributions:  $\mathcal{N}$  stands for a univariate normal and  $\mathcal{N}_N$  stands for the  $N$ -variate normal distribution.  $\mathcal{NP}$  stands for a univariate normal product while  $\log \mathcal{NP}$  for the univariate log normal product distribution (to be defined in Section 3). The gamma distribution is denoted by  $\mathcal{G}$ , the inverted gamma 2 by  $\mathcal{IG2}$ , and the uniform distribution by  $\mathcal{U}$ . Unless specified otherwise,  $n$  goes from 1 to  $N$ ,  $t$  goes from 1 to  $T$ , and  $s$  goes from 1 to  $S$ .

## 2. Two approaches to parameterize stochastic volatility in SVARs

We begin with the following reduced-form VAR model of order  $p$ :

$$\mathbf{y}_t = \mathbf{A}_1 \mathbf{y}_{t-1} + \cdots + \mathbf{A}_p \mathbf{y}_{t-p} + \mathbf{A}_d \mathbf{d}_t + \mathbf{u}_t, \quad (2.1)$$

where  $\mathbf{y}_t$  is an  $N$ -dimensional vector of observable time series variables,  $\mathbf{A}_i$ ,  $i = 1, \dots, p$ , are  $N \times N$  autoregressive coefficient matrices,  $\mathbf{d}_t$  is a  $d \times 1$  vector containing deterministic terms such as the intercept, trend variables, or dummies,  $\mathbf{A}_d$  is the corresponding  $N \times d$  matrix of coefficients, and  $\mathbf{u}_t = (u_{1,t}, \dots, u_{N,t})'$  is an  $N$ -dimensional, zero-mean, serially uncorrelated error term.

The structural form links the reduced-form innovations  $\mathbf{u}_t$  to the structural shocks  $\mathbf{w}_t$

via the  $N \times N$  contemporaneous effects matrix  $\mathbf{B}_0$ :

$$\mathbf{B}_0 \mathbf{u}_t = \mathbf{w}_t, \quad (2.2)$$

where the structural shocks are contemporaneously uncorrelated. Their (possibly time-varying) unconditional or conditional variances are collected in the diagonal matrix

$$\mathbf{\Lambda}_t = \text{diag}(\sigma_{1,t}^2, \dots, \sigma_{N,t}^2), \quad (2.3)$$

so that the unconditional or conditional covariance matrices of the reduced-form errors are  $\mathbf{\Sigma}_t = \mathbb{E}[\mathbf{u}_t \mathbf{u}_t']$  or  $\mathbb{E}[\mathbf{u}_t \mathbf{u}_t' \mid \mathbf{u}_{t-1}, \mathbf{u}_{t-2}, \dots]$ , respectively.

It is well-known that the structural matrix  $\mathbf{B}_0$  is not identified without additional restrictions. Theorem A.1 in the Appendix provides general conditions for partial identification of individual rows of  $\mathbf{B}_0$  in settings where heteroskedasticity supplies the identifying variation. The Theorem states that a structural shock is identified if a sequence of its appropriately scaled (conditional) variances is different from the corresponding sequences of (conditional) variances of all other shocks. These conditions are closely related to those presented by [Lütkepohl and Woźniak \(2020\)](#) in the context of Markov-switching heteroskedasticity. In particular, our setup generalizes [Lütkepohl and Woźniak \(2020\)](#) by allowing volatility changes at every point in time, rather than restricting them to a finite number of regimes. For conciseness, Theorem A.1 is reported in the Appendix, but we will refer to it throughout the paper as needed.

We now shift our focus to heteroskedastic SVARs, where shocks are modeled and identified through stochastic volatility. Specifically, we examine two parameterizations of this process: the centred and non-centred approaches.

#### *The centred parameterization*

To fix ideas, we first present the more conventional (centred) parameterization for modeling stochastic volatility. In this setup, each diagonal element of  $\mathbf{\Lambda}_t$  in (2.3) is

parameterized as follows:

$$\sigma_{n,t}^2 = \exp(\tilde{h}_{n,t}), \quad (2.4)$$

$$\tilde{h}_{n,t} = \rho_n \tilde{h}_{n,t-1} + \tilde{v}_{n,t} \quad \text{s.t.} \quad \rho_n \in (-1, 1), \quad (2.5)$$

$$\tilde{v}_{n,t} \sim \mathcal{N}(0, \omega_n^2) \quad \text{for } n = 1, \dots, N \text{ and } t = 1, \dots, T. \quad (2.6)$$

This model is often complemented by an inverse-gamma prior for  $\omega_n^2$  (see [Primiceri, 2005](#); [Cogley and Sargent, 2005](#); [Clark and Ravazzolo, 2015](#); [Carriero et al., 2016](#); [Chan et al., 2024](#), and others). Theorem A.1 implies that identification depends on the sequence of conditional variances,  $\{\sigma_{n,t}^2\}_{t=1}^T$ , associated with a shock. The shock is identified if its conditional variance sequence is not proportional to any sequence of volatilities from another shock in the system. These conditions are satisfied under (2.4)–(2.6), as this representation assumes that the log-volatility state variable  $\tilde{h}_{n,t}$  (and thus  $\sigma_{n,t}^2$ ) evolves stochastically as a stationary autoregressive process.

In this setup, assessing identification through stochastic volatility reduces to testing whether  $\omega_n^2 = 0$ . If that is the case, the corresponding shock is homoskedastic and is identified only if all other  $\omega_k^2 \neq 0$ ,  $n \neq k$ . Conversely, if  $\omega_n^2 \neq 0$ , then by construction  $\{\sigma_{n,t}^2\}_{t=1}^T$  is unique, and the condition for identification in Theorem A.1 is satisfied.

Nevertheless, implementing statistical tests for  $\omega_n^2 = 0$  is challenging because zero lies at the boundary of the parameter space for  $\omega_n^2$ . Moreover, Bayesian methods that estimate stochastic volatility models under the centred parameterization typically use an inverse-gamma prior for  $\omega_n^2$ , whose domain is undefined at zero. To address these issues, we adopt the non-centred parameterization for  $\sigma_{n,t}^2$ , discussed next.

#### *The non-centred parameterization*

To obtain the non-centred parameterization of  $\sigma_{n,t}^2$ , akin to [Kastner and Frühwirth-Schnatter \(2014\)](#) and [Chan \(2018\)](#), we first define  $\tilde{h}_{n,t} = \omega_n h_{n,t}$ . This transforms

(2.4)–(2.6) into

$$\sigma_{n,t}^2 = \exp(\omega_n h_{n,t}), \quad (2.7)$$

$$h_{n,t} = \rho_n h_{n,t-1} + v_{n,t} \quad \text{s.t.} \quad \rho_n \in (-1, 1), \quad (2.8)$$

$$v_{n,t} \sim \mathcal{N}(0, 1) \quad \text{for } n = 1, \dots, N \text{ and } t = 1, \dots, T. \quad (2.9)$$

We further assume that  $h_{n,0} = 0$ , ensuring  $\sigma_{n,0}^2 = 1$  to satisfy the normalization condition in Theorem A.1.

Importantly, the conditions in Theorem A.1 hold under more general specifications for the covariance structure of the innovations, that is, when the innovations driving  $h_{n,t}$  and  $\tilde{h}_{n,t}$  are correlated, given that correlation does not imply proportionality of  $\{\sigma_{n,t}^2\}_{t=1}^T$  across equations. Even perfect correlation of volatility shocks  $v_{n,t}$  and  $\tilde{v}_{n,t}$  does not imply proportional changes of the conditional variances  $\sigma_{n,t}^2$  due to the non-linear transformation in Equations (2.7) and (2.4), respectively. This proportionality arises only when the shocks are perfectly correlated, parameters  $\rho_n$  and  $\omega_n^2$  are equal to their counterparts across equations, and  $\omega_n^2 \neq 0$ , an extreme scenario excluded in our framework.

While there is a one-to-one mapping between the representations in (2.4)–(2.6) and (2.7)–(2.9), they have markedly different implications for (i) the marginal prior distribution of  $\sigma_{n,t}^2$  and (ii) the feasibility of proposing a statistical method to assess shock identification. These implications are elaborated in Sections 3 and 4.

Two more comments are in order. First, unlike the centred parameterization, the non-centred representation for  $\sigma_{n,t}^2$  is cast in terms of the standard deviation parameter  $\omega_n$  instead of  $\omega_n^2$ . Given that  $\omega_n$  can take both positive and negative values on a real line, the non-centred approach allows us to elicit priors for which  $\omega_n$  is defined at zero. As shown later in Section 3.1, we propose a conditionally normal prior for  $\omega_n$  centred at zero, which implies a gamma prior for  $\omega_n^2$ . The gamma prior allocates more mass near  $\omega_n^2 = 0$  compared to the inverse-gamma prior typically used in the centred approach (see Chan, 2018). Consequently, the non-centred approach enables stronger shrinkage toward homoskedasticity also providing normalisation of the conditional variances

around value 1.

Second, it is easy to see from (2.7) that the likelihood function is invariant to sign at the  $(\omega_n, h_{n,t})$  ordinate. This follows from the fact that both  $(\omega_n, h_{n,t})$  and  $(-\omega_n, -h_{n,t})$  yield the same value for  $\sigma_{n,t}^2$ . Consequently, the posterior for  $\omega_n$  may be bimodal or unimodal around zero. Bimodality will only occur if  $\omega_n$  (and, consequently  $\omega_n^2$ ) is far from zero. Therefore, bimodality of the posterior for  $\omega_n$  provides evidence that  $\sigma_{n,t}^2 \neq 0$ , supporting the identification of structural shocks through stochastic volatility. For the purpose of identification, a bimodal (as opposed to unimodal) posterior for  $\omega$  is desirable. We return to this point in the context of our empirical application in Section 6.

Having distinguished two approaches to model  $\sigma_{n,t}^2$ , for the remainder of this paper, we adopt the non-centred parameterization unless explicitly stated otherwise.

### 3. The marginal prior for $\sigma_{n,t}^2$

In the context of Bayesian estimation,  $\sigma_{n,t}^2$  can be characterized through its marginal prior distribution. However, as shown in the previous section,  $\sigma_{n,t}^2$  is a non-linear function of  $h_{n,t}$ ,  $\omega_n$ , and  $\rho$ . This non-linearity complicates the assessment of how the choice of priors for these variables affects the marginal prior for  $\sigma_{n,t}^2$ .

To shed light on this matter, this section provides a detailed examination of the marginal prior for  $\sigma_{n,t}^2$ . This is achieved in two steps. First, the priors for the parameters that underlie  $\sigma_{n,t}^2$ , namely  $\omega_n$  and  $\rho$ , are specified. Second, the proposed marginal prior for  $\sigma_{n,t}^2$  is characterized, illustrating how it ensures centring and shrinkage towards a homoskedastic SVAR. In what follows, we focus on the characterization of a univariate prior for  $\sigma_{n,t}^2$  and provide more general results for a multivariate distribution of  $\{\sigma_{n,t}^2\}_{t=1}^T$  in Supplementary Materials.

#### 3.1. Priors for the parameters underlying $\sigma_{n,t}^2$

Once again, the parameters associated with the non-centred representation of  $\sigma_{n,t}^2$  are  $\omega_n$ , the essential parameter in our setup that determines whether  $\sigma_{n,t}^2$  changes over time,

and  $\rho_n$ , the autoregressive parameter of the latent process  $h_{n,t}$ . We assume the following hierarchical prior structure for these parameters:

$$\omega_n \mid \sigma_{\omega_n}^2 \sim \mathcal{N}(0, \sigma_{\omega_n}^2), \quad (3.1)$$

$$\sigma_{\omega_n}^2 \mid \rho_n \sim \mathcal{G}(\underline{S}, \underline{A}) \mathcal{I}(0 < \sigma_{\omega_n}^2 < 1 - \rho_n^2), \quad (3.2)$$

$$\rho_n \mid \sigma_{\omega_n}^2 \sim \mathcal{U}\left(-\sqrt{1 - \sigma_{\omega_n}^2}, \sqrt{1 - \sigma_{\omega_n}^2}\right), \quad (3.3)$$

where  $\sigma_{\omega_n}^2$  denotes the prior variance of  $\omega_n$ .

The prior specification for  $\omega_n$  in (3.1) extends the one proposed by Chan (2018). Specifically, instead of fixing the prior variance as in Chan (2018), we adopt a hierarchical prior in which  $\sigma_{\omega_n}^2$  follows the gamma distribution stated in (3.2). Consequently, our specification allows for the estimation of  $\sigma_{\omega_n}^2$ , making the prior for  $\omega_n$  less dependent on arbitrary choices. Moreover, based on the results of Bitto and Frühwirth-Schnatter (2019) and Cadonna, Frühwirth-Schnatter, and Knaus (2020), marginalizing the prior for  $\omega_n$  over  $\sigma_{\omega_n}^2$  yields a prior that combines extreme shrinkage towards homoskedasticity with heavy tails. The latter accommodates heteroskedasticity when it arises from strong data signals.

We complement the three priors above with the following three restrictions:

$$\frac{\sigma_{\omega_n}^2}{1 - \rho_n^2} \leq 1, \quad (3.4)$$

$$\underline{A} > 0.5, \quad (3.5)$$

$$|\rho_n| < 1. \quad (3.6)$$

Restriction (3.4) ensures the desired level of centring and shrinkage in our proposed marginal prior for  $\sigma_{n,t}^2$ , which we show formally in Section 3.2. It restricts the prior variances from Proposition 1 presented below in the limit  $\lim_{t \rightarrow \infty} \sigma_{\omega_n}^2 \frac{1 - \rho_n^{2t}}{1 - \rho_n^2} = \sigma_{\omega_n}^2 / (1 - \rho_n^2)$  to ensure that the condition holds for variances at all periods  $t$ . The restriction in (3.5) determines the marginal prior for  $\omega_n$ , making it particularly suitable for our setup.

Restriction (3.6) is standard and ensures that  $h_{n,t}$  in (2.8) is stationary. Additionally, Restrictions (3.6) and (3.4) determine the bounds for  $\rho_n$  as expressed in the uniform prior for  $\rho_n$  in (3.3). Similarly, the truncation of the gamma prior for  $\sigma_{\omega_n}^2$  stated in (3.2) arises from Restriction (3.4). We provide further elaboration on these restrictions later in this section.

### 3.2. Characterizing the marginal prior for $\sigma_{n,t}^2$

This section provides a detailed description of the marginal prior for  $\sigma_{n,t}^2$ . As discussed in the Introduction, a key feature of our prior setup for  $\sigma_{n,t}^2$  is to ensure that this prior is not only centred on the hypothesis of a homoskedastic SVAR but also provides shrinkage toward it. In this regard, Definitions 1 and 2, along with Proposition 1, presented below, will be instrumental in structuring the approach to achieving these objectives.

#### **Definition 1. Normal product distribution**

Let  $x$  and  $y$  denote two independent zero-mean normally distributed random variables with variances  $\sigma_x^2$  and  $\sigma_y^2$ , respectively. Then, random variable  $z = xy$  follows the normal product distribution with zero mean and variance  $\sigma_z^2 = \sigma_x^2\sigma_y^2$ , denoted by  $z \sim \mathcal{NP}(\sigma_z^2)$ , and density function given by  $\frac{1}{\pi\sqrt{\sigma_z^2}}K_0\left(\frac{|z|}{\sqrt{\sigma_z^2}}\right)$ .  $\square$

The normal product distribution is known in the statistical literature. We state it here to clarify our notation. However, the following distribution is new and its density function is obtained by a change of variables.

#### **Definition 2. Log-normal product distribution**

Let random variable  $z$  follow the normal product distribution with variance  $\sigma_z^2$ . Then, random variable  $q = \exp(z)$  follows the log-normal product distribution, denoted  $q \sim \log \mathcal{NP}(\sigma_z^2)$ , with density given by:  $\frac{1}{\pi\sqrt{\sigma_z^2}q}K_0\left(\frac{|\log q|}{\sqrt{\sigma_z^2}}\right)$ .  $\square$

Based on the results from Definitions 1 and 2, we can state Proposition 1:

**Proposition 1. Auxiliary results on conditional distributions for  $h_{n,t}$  and  $\sigma_{n,t}^2$**  Given the prior specification from Equations (2.7)–(2.6) and (3.1)–(3.5), the marginal priors for the latent process  $h_{n,t}$ , log-conditional variances  $\log \sigma_{n,t}^2 = \omega_n h_{n,t}$ , and conditional variances  $\sigma_{n,t}^2 = \exp(\omega_n h_{n,t})$  are given by the following normal, normal product, and log normal product distributions:

(a)  $h_{n,t} \mid \rho_n \sim \mathcal{N}\left(0, \frac{1-\rho_n^{2t}}{1-\rho_n^2}\right)$ ,

(b)  $\log \sigma_{n,t}^2 \mid \rho_n, \sigma_{\omega_n}^2 \sim \mathcal{NP}\left(\sigma_{\omega_n}^2 \frac{1-\rho_n^{2t}}{1-\rho_n^2}\right)$ ,

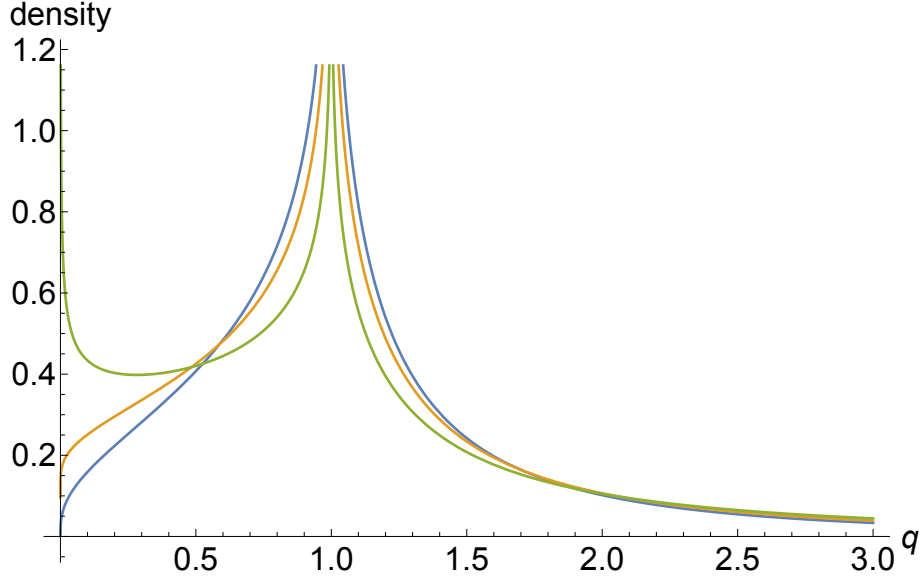
(c)  $\sigma_{n,t}^2 \mid \rho_n, \sigma_{\omega_n}^2 \sim \log \mathcal{NP}\left(\sigma_{\omega_n}^2 \frac{1-\rho_n^{2t}}{1-\rho_n^2}\right)$ .

*Proof.* (a) The result is based on the properties of a normal compound distribution that facilitates the integration of  $\int p(h_{n,t}, h_{n,t-1}, \dots, h_{n,1}) d(h_{n,t-1}, \dots, h_{n,1})$ , where the joint distribution under the integral is constructed from the conditional distributions  $h_{n,t} \mid h_{n,t-1}, \dots, h_{n,1} \sim \mathcal{N}(\rho_n h_{n,t-1}, 1)$  and using  $h_{n,0} = 0$ . (b) The result is obtained directly by applying Definition 1, the result (a) and the prior in Expression (3.1). Point (c) is obtained as a straightforward consequence of the first two results and Definition 2.  $\square$

The introduced results facilitate centring and shrinking our prior for  $\sigma_{n,t}^2$  toward a homoskedastic SVAR, which is useful because it ensures that evidence supporting heteroskedasticity – and, consequently, the identification of a shock – must come from the data. Moreover, it provides an alternative strategy for normalizing SVARs that does not rely on common approaches, such as setting the diagonal elements of  $\mathbf{B}_0$  to one or imposing that the expected value of  $\sigma_{n,t}^2$  equals one. Both of these approaches complicate the derivation of an efficient Bayesian estimation algorithm. In what follows, we discuss how we achieve centring and shrinking of our prior for  $\sigma_{n,t}^2$ .

To centre the prior for  $\sigma_{n,t}^2$  around the hypothesis of homoskedasticity, we must ensure that the log-normal product distribution characterizing  $\sigma_{n,t}^2$  has a single pole at the value 1. This follows directly from two points: (i) the normalization condition in Theorem A.1, which sets  $\sigma_{n,0}^2 = 1$ , and (ii) the fact that homoskedasticity in our setup corresponds to setting  $\omega_n = 0$ , which implies  $\sigma_{n,t}^2 = \exp(\omega_n h_{n,t}) = 1$ , as discussed in Section 2. Property 1,

Figure 1: Densities of the log-normal product distribution for various values of the scale parameter.



Note: The blue, orange, and green lines correspond to the densities for the values of the scale parameter  $\sigma_z^2$  equal to 0.8, 1, and 1.5, respectively.

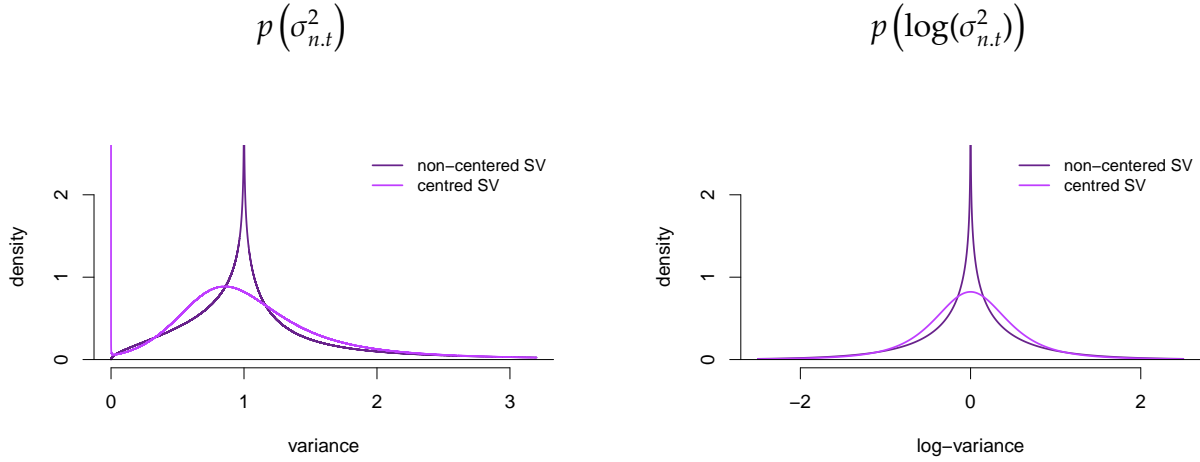
presented below, establishes when the log-normal product for  $\sigma_{n,t}^2$  is proper and has a single pole at 1.

**Property 1. Single pole of log-normal product distribution at point 1**

The log-normal product distribution from Definition 2 has a single pole at point 1 when its variance satisfies  $\sigma_z^2 \leq 1$ . In this case, the value of the density function approaches infinity when its argument,  $q$ , goes to 1 and approaches 0 when  $q$  goes to 0 from the right. If  $\sigma_z^2 > 1$ , this distribution has an additional pole at 0, hence approaching infinity as  $q$  goes to either 0 or 1.

Figure 1 illustrates Property 1. A few points are worth highlighting. First, note that the condition for a single pole at one was stated in (3.4), which denotes a restriction on the variance of the prior limiting distribution for  $\sigma_{n,t}^2$ , as characterized in Proposition 1. This restriction ensures that the inequality in (3.4) holds for all  $t$ . Second, the single-pole-at-one condition implies a strong concentration of the prior probability mass for  $\sigma_{n,t}^2$  at the value corresponding to the homoskedasticity of the structural shocks. This prior is equation

Figure 2: The marginal priors for  $\sigma_{n,t}^2$  and  $\log(\sigma_{n,t}^2)$  in their centred and non-centred parameterizations



Note: The densities above correspond to the non-centred and centred approaches to model  $\sigma_{n,t}^2$ , as discussed in Section 2.

invariant and, thus, it supports our claim that, at the prior mode, the SVAR model is not identified through heteroskedasticity.

The prior shrinkage for  $\sigma_{n,t}^2$  is also achieved through Property 1 via the inequality restriction in (3.4). Specifically, this restriction prevents the prior probability mass for  $\sigma_{n,t}^2$  from being distributed more evenly over the interval from 0 to 1, as would occur in the presence of an additional pole at zero as for the density plotted in green in Figure 1.

The centering and shrinkage effects resulting from our prior setup are more evident in Figure 2, which compares the marginal prior distributions for  $\sigma_{n,t}^2$  and  $\log(\sigma_{n,t}^2)$  based on their centred and non-centred parameterizations.<sup>2</sup>

Notably, the marginal prior for  $\sigma_{n,t}^2$  in the non-centred case inherits the properties from the log-normal product conditional prior for  $\sigma_{n,t}^2$  given  $\rho_n$  and  $\sigma_{\omega_n}^2$ , stated in Proposition 1(c) with a less-than-one restriction on its variance from Expression (3.4). These properties

<sup>2</sup>The marginal priors in Figure 2 are computed using the numerical integration of Gelfand and Smith (1990) in two steps. In the first one for the non-centred parameterization, a sample of  $S$  draws is obtained from the prior distributions, denoted by  $\{\rho_n^{(s)}, \sigma_{\omega_n}^{2(s)}\}_{s=1}^S$ . In the second step, the marginal prior ordinates at pre-specified points, denoted by  $\zeta_g$  for  $g = 1, \dots, G$ , are each computed by  $\widehat{p}(\sigma_{n,t}^2 = \zeta_g) = S^{-1} \sum_{s=1}^S p(\sigma_{n,t}^2 = \zeta_g | \rho_n^{(s)}, \sigma_{\omega_n}^{2(s)})$ . Appropriate modifications reflecting the prior assumptions are made for the centred parameterization computations.

are convergence to value zero when the conditional variance goes to zero from the right, a pole at 1, strong shrinkage toward the prior mode, and heavy tails.

In contrast, in the centred case, the marginal prior for  $\sigma_{n,t}^2$  has the properties of the log-Student-t distribution revisited in Supplementary Materials, that is, less concentration around the hypothesis of homoskedasticity, a mode at one, and a pole at zero. This log-Student-t distribution arises from the inverse gamma prior for  $\omega_n^2$  featured by the centred parameterization and the exponential transformation of the log-volatility to conditional variance. In summary, the prior distribution for  $\sigma_{n,t}^2$  in the centred parameterization favours heteroskedasticity, implies shock identification even in the absence of time-varying volatility, and does not support the normalization of the conditional variances at one.

#### 4. Bayesian Verification of Identification

Recall from Section 2 that in our non-centred setup, identifying a given shock  $n$  thorough heteroskedasticity involves assessing the restriction  $\omega_n = 0$ . If this restriction holds, then  $h_{n,t} = 0$  and  $\sigma_{n,t}^2 = 1$  for all  $t$ , which corresponds to a homoskedastic shock. Conversely, if  $\omega_n \neq 0$ , then the conditions in Theorem A.1 ensure shock identification through heteroskedasticity.

To assess  $\omega_n = 0$ , we adopt a Bayesian approach by comparing the fit of homoskedastic and a partially heteroskedastic SVAR using the Bayes factor. To compute the Bayes factor, we use the SDDR approach, which defines the Bayes factor as

$$BF_{homosk} = \frac{p(\omega_n = 0 | \mathbf{y})}{p(\omega_n \neq 0)}. \quad (4.1)$$

The numerator in (4.1) is computed using numerical integration methods based on the estimator proposed by Gelfand and Smith (1990). This approach only requires the full conditional posterior distribution of  $\omega_n$  to be known up to its probability density function, which is normal, and the posterior draws from the unrestricted model ( $\omega_n \neq 0$ ). Consequently, computation of (4.1) requires estimation only under the unrestricted, that

is, heteroskedastic SVAR. Supplementary Materials provide a detailed description of the evaluation of the marginal posterior density  $p(\omega_n = 0|\mathbf{y})$ .

The denominator  $p(\omega_n = 0)$  involves the marginal prior, which is obtained by integrating out  $\sigma_{\omega_n}^2$  from the hierarchical-prior structure of  $\omega_n$ , discussed in Section 3.1, where  $\omega_n|\sigma_{\omega_n}^2 \sim \mathcal{N}(0, \sigma_{\omega_n}^2)$  and  $\sigma_{\omega_n}^2 \sim \mathcal{G}(\underline{S}, \underline{A})$ . Proposition 2 formalizes this marginal prior as follows:

**Proposition 2. Density of the marginal prior  $p(\omega_n)$**  *The marginal prior density function for parameter  $\omega_n$  obtained by marginalizing the joint prior distribution  $p(\omega_n, \sigma_{\omega_n}^2)$  over  $\sigma_{\omega_n}^2$ ,  $p(\omega_n) = \int_0^\infty p(\omega_n | \sigma_{\omega_n}^2) p(\sigma_{\omega_n}^2) d\sigma_{\omega_n}^2$ , where the priors  $p(\omega_n | \sigma_{\omega_n}^2)$  and  $p(\sigma_{\omega_n}^2)$  are given by Expressions (3.1) and (3.2), respectively. This yields*

$$p(\omega_n) = \frac{|\omega_n|^{\underline{A}-\frac{1}{2}} K_{\underline{A}-\frac{1}{2}}\left(\sqrt{\frac{2}{\underline{S}}}|\omega_n|\right)}{\sqrt{\pi}\left(\sqrt{2}\right)^{\underline{A}-\frac{3}{2}}\Gamma(\underline{A})\left(\sqrt{\underline{S}}\right)^{\underline{A}+\frac{1}{2}}}. \quad (4.2)$$

□

*Proof.* The integration proceeds by recognizing the constant and kernel and applies to the latter, which is facilitated using the normalizing constant of the generalized inverse Gaussian distribution provided by [Barndorff-Nielsen \(1997\)](#). □

To compute the Bayes factor using the SDDR approach, it is crucial that the marginal prior  $p(\omega_n)$  is bounded at  $\omega_n = 0$ . Property (2) establishes that the existence of this bound depends on the hyperparameter  $\underline{A}$ :

**Property 2. Upper bound of the marginal prior density for  $\omega_n$**  (see [Cadonna et al., 2020](#), Theorem 2).

$$\lim_{\omega_n \rightarrow 0} p(\omega_n) = \begin{cases} \infty & \text{for } 0 < \underline{A} \leq 0.5, \\ \frac{1}{\sqrt{2\pi\underline{S}}\left(\underline{A}^2 - \frac{1}{4}\right)} \frac{\Gamma\left(\underline{A} + \frac{3}{2}\right)}{\Gamma(\underline{A})} & \text{for } \underline{A} > 0.5. \end{cases} \quad (4.3)$$

Thus, the marginal prior density  $p(\omega_n)$  is bounded from above if  $\underline{A} > 0.5$ , as required by Restriction (3.5). Accordingly, we set  $\underline{A} = 1$ , reducing the gamma prior to an exponential distribution, consistent with the Bayesian Lasso prior considered by Belmonte, Koop, and Korobilis (2014). Other choices are possible and are reviewed by Cadonna et al. (2020). Additionally, we set the hyper-parameter  $\underline{S} = 0.05$ , ensuring that nearly all prior probability mass for  $\sigma_{\omega_n}^2$  lies within the interval  $(0, 1)$ .

## 5. Two Monte Carlo studies

In light of our new methods, practitioners may wonder about our model’s ability to normalize the system, effectively estimate the structural parameters, and verify structural shocks in finite samples under a misspecified variance process. To address these questions, we conduct two comparative Monte Carlo (MC) studies. The first investigates the estimation efficiency of key parameters for partial identification under heteroskedasticity, namely, selected rows of the structural matrix ( $\mathbf{B}_0$ ) and conditional variances of the structural shocks ( $\sigma_{n,t}^2$ ). The second assesses the performance of our verification procedure for shock identification in Section 4 under different volatility processes. To implement these exercises, we rely on the posterior simulation algorithm, with details provided in Supplementary Materials.

### 5.1. Estimation efficiency under centred and non-centred stochastic volatility

We highlight that the centred parameterization may fail to normalize SVARs—that is, to distinguish between  $\mathbf{B}_0$  and  $\sigma_{n,t}^2$ —due to the hump-shaped, as opposed to shrinking, prior for  $\sigma_{n,t}^2$  centred around one, as illustrated in Figure 2. This could cause distortions in the parameter estimates of both  $\mathbf{B}_0$  and  $\sigma_{n,t}^2$ . Therefore, using simulated data, we investigate whether the non-centred approach improves the estimation accuracy of  $\mathbf{B}_0$  and  $\sigma_{n,t}^2$ , and consequently enhances system normalization.

Specifically, our first MC exercise simulates 100 artificial datasets from six different data-generating processes (DGPs), which vary by system dimension  $N$  and sample length  $T$ . For each dataset, we estimate SVAR-SVs under both centred and non-centred

parameterizations of  $\sigma_{n,t}^2$  to assess estimation precision. We measure accuracy using root-mean-squared errors (RMSEs). The DGPs include systems with  $N \in \{3, 10, 20\}$  variables, matching the dimensions considered in our empirical application in Section 6 and related VAR studies. We set the sample sizes to  $T \in \{260, 780\}$ , corresponding to 65 years of quarterly and monthly data, respectively. To focus on identification, we use a simplified DGP that ignores the SVAR's autoregressive coefficients and concentrates on the structural matrix  $\mathbf{B}_0$  and the conditional variances  $\sigma_{n,t}^2$ . The DGP for this exercise is thus given by:

$$\mathbf{B}_0 \mathbf{y}_t = \mathbf{w}_t, \quad \mathbf{w}_t \sim \mathcal{N}_N(\mathbf{0}_N, \text{diag}(\sigma_t^2)), \quad (5.1)$$

$$\sigma_{n,t}^2 = \exp(0.5h_{n,t}), \quad h_{n,t} = 0.92h_{n,t-1} + v_{n,t}, \quad v_{n,t} \sim \mathcal{N}(0, 0.25). \quad (5.2)$$

For a three-variable system, we set  $\mathbf{B}_0$  to [Blanchard and Perotti's](#) estimates. We extend it to ten- and twenty-variable systems by filling the remaining diagonal elements with random draws from a gamma distribution with mean 100 and variance 1000, and by filling the lower-diagonal elements with random draws from a zero-mean normal distribution with variance 4. The stochastic volatility process in (5.2) reproduces the relatively high volatility persistence observed in macroeconomic aggregates and, with fixed parameters, represents both the centred and non-centred volatility specifications. We then estimate the structural models in (5.1) using both the centred and non-centred volatility formulations, maintaining similar priors across the two specifications.

Table 1 reports the relative RMSEs for  $\mathbf{B}_0$  and  $\sigma_{n,t}$  for the first three equations in all systems. We calculate the errors as the difference between the posterior mean estimates and the corresponding values of the data-generating processes. The RMSEs include all elements from the first three rows of the structural matrix and the conditional standard deviations for the first three equations across all periods. We compute the relative RMSEs with the non-centred specification in the numerator and the centred specification in the denominator. Hence, values below one indicate superior estimation accuracy for the non-centred version.

Table 1: Relative RMSEs of non-centred vs. centred stochastic volatility specifications

$N$	$\mathbf{B}_0$		$\sigma_{n,t}$	
	$T$		$T$	
	260	780	260	780
3	0.883	0.743	0.907	0.846
10	0.934	0.723	0.948	0.853
20	0.947	0.778	0.952	0.896

Note: The table reports the ratios of the overall root-mean-squared error for structural matrix,  $\mathbf{B}_0$ , and conditional standard deviations,  $\sigma_{n,t}$ , for  $t = 1, \dots, T$ . We report root-mean-squared errors for the parameters from the first three equations in all the systems with  $N = 3, 10$ , and 20 variables. The values of ratios less than 1 indicate that the parameters in our SVAR model with non-centred SV are estimated more precisely than in the model with centred SV.

The results for  $\mathbf{B}_0$  show that the non-centred specification consistently outperforms the centred one in terms of RMSE. This difference matters because the structural parameters determine quantities such as impulse responses and forecast error variance decompositions. RMSE reductions for the non-centred specification range from about 5% for the shorter sample ( $T = 260$ ) to around 22% for the longer sample ( $T = 720$ ), and tend to decrease as the system dimension  $N$  increases for a given sample size. Supplementary Materials report RMSE results for individual parameters in the top-left  $3 \times 3$  block of  $\mathbf{B}_0$ , showing that most parameters exhibit similar improvements across the different DGPs.

The results for  $\sigma_{n,t}$  show similar patterns. Table 1 reports RMSE reductions ranging from about 5% in the short sample ( $T = 260$ ) to roughly 10% in the longer sample ( $T = 780$ ). These gains tend to increase slightly as the system dimension  $N$  decreases for a given sample size. Supplementary Materials present additional results indicating that the improvements hold across all periods in the simulated data. Overall, these findings highlight the ability of the non-centred specification to more accurately normalize SVAR-SVs and support its empirical suitability in both smaller and larger models.

## 5.2. Assessing the verification procedure for partial identification

As discussed in Section 4, verifying whether a shock is partially identified boils down to testing for homoskedasticity. To explore how well the SDDR procedure detects homoskedastic shocks, our second MC exercise evaluates its performance under two alternative prior specifications for  $\omega_n$ : (i) our hierarchical prior structure in (3.1)–(3.3), and (ii) the zero-mean normal prior with fixed variance  $\sigma_{\omega_n}^2 = 10$  proposed by Chan (2018). The latter violates the scaling restriction in (3.4), potentially affecting normalization.<sup>3</sup> For this analysis, we implement the SDDR procedure using the non-centred parameterization of a system with stochastic volatility under both prior specifications.

We assess these priors by estimating the models on multiple artificially generated datasets. All DGPs in this exercise are bivariate and follow the structural equation (5.1), with the structural matrix  $\mathbf{B}_0$  chosen to reflect parameter estimates from our empirical application in Section 6. The only variation across DGPs is in the volatility process, for which we consider three alternative specifications:

**SV:** following the specification in (5.2).

**GARCH:** where  $\sigma_{n,t}^2 = 0.02 + 0.28u_{n,t-1}^2 + 0.7\sigma_{n,t-1}^2$  and  $\sigma_{n,0}^2 = 1$ .

**Markov switching heteroskedasticity (MSH):** where  $\sigma_{n,t}^2 = \sigma_{n,s_t}^2$ ,  $s_t$  is a two-state Markov process with transition probabilities  $\mathbf{P} = \begin{bmatrix} 0.98 & 0.02 \\ 0.02 & 0.98 \end{bmatrix}$ , for  $s_t = 1$ ,  $\mathbf{w}_t \sim \mathcal{N}(\mathbf{0}_2, I_2)$  and for  $s_t = 2$ ,  $\mathbf{w}_t \sim \mathcal{N}(\mathbf{0}_2, \text{diag}(20, 10))$ .

Clearly, only the first volatility specification corresponds to our Bayesian verification of identification procedure in Section 4, which implies that this procedure is violated when volatility changes follow either of the other two models. In other words, our second MC exercise provides a way to assess the robustness of our approach to misspecification.

---

<sup>3</sup>We note, however, that the prior for  $\omega_n$  in Chan (2018) was implemented within a reduced-form setup, where normalization is less of a concern.

Table 2: Simulation results: rejection rates for homoskedasticity using our prior vs. [Chan \(2018\)](#)

		Our prior			Chan (2018) prior		
$T$	homoskedastic shocks in each DGP	DGPs			DGPs		
		SV	GARCH	MSH	SV	GARCH	MSH
Panel A: $l$ -value approach							
260	shocks 1 & 2	0.00	0.00	0.00	0.00	0.00	0.00
	shock 1	0.01	0.01	0.00	0.02	0.00	0.01
	shock 2	0.57	0.31	0.19	0.55	0.27	0.30
	none	0.78	0.37	0.41	0.74	0.28	0.61
780	shocks 1 & 2	0.00	0.00	0.00	0.00	0.00	0.00
	shock 1	0.00	0.00	0.02	0.01	0.00	0.01
	shock 2	0.98	0.80	0.22	0.95	0.71	0.18
	none	1.00	0.83	0.56	0.98	0.73	0.49
Panel B: $q$ -value approach							
260	shocks 1 & 2	0.05	0.05	0.05	0.05	0.05	0.05
	shock 1	0.07	0.12	0.10	0.07	0.10	0.07
	shock 2	0.85	0.55	0.37	0.82	0.59	0.39
	none	0.95	0.68	0.78	0.96	0.69	0.78
780	shocks 1 & 2	0.05	0.05	0.05	0.05	0.05	0.05
	shock 1	0.08	0.13	0.09	0.07	0.11	0.10
	shock 2	0.99	0.94	0.53	0.99	0.94	0.54
	none	1.00	0.97	0.91	1.00	0.98	0.90

Note: The table reports rejection rates for the hypothesis of homoskedasticity in the first shock, i.e.,  $\mathcal{H}_0 : \omega_1 = 0$  using simulated data. The rates are calculated based on 100 realizations of DGPs each with the following characteristics: sample sizes:  $T \in \{260, 780\}$ ; volatility processes: SV, GARCH, MSH; homoskedastic shock arrangements: shocks 1 & 2, shock 1, shock 2, none. For a homoskedastic shock, the variance is set to  $\sigma_{\eta}^2 = 1$ .

For each volatility process, we generate data using four different scenarios: (1) both shocks are homoskedastic, (2) the first shock is homoskedastic while the second shock is heteroskedastic, (3) the first shock is heteroskedastic while the second shock is homoskedastic, (4) both shocks are heteroskedastic. For homoskedastic shocks we set

$\sigma_{n,t}^2 = 1$  for all  $t$ , while the heteroskedastic shocks are generated by the two different volatility models. Akin to the first MC exercise, we consider two sample sizes,  $T \in \{260, 780\}$ , and generate 100 simulated datasets for each of the four shock scenarios described above.

Table 2 reports rejection rates for testing the homoskedasticity of the first shock. These rates are obtained using two strategies for constructing critical values, which we label  $l$ -value and  $q$ -value following [Benjamini and Hochberg \(1995\)](#) and [Storey \(2002\)](#). In the  $l$ -value approach (Panel A), we apply a decision-theoretic rule and reject homoskedasticity if  $BF_{homosk} < 1$ , where  $BF_{homosk}$  is defined in Equation (4.1); that is, rejection occurs when the posterior assigns more than 50% probability to heteroskedasticity. In the  $q$ -value approach (Panel B), the critical value corresponds to the fifth percentile of the posterior odds ratio  $BF_{homosk}$  computed under the null  $\omega_1 = 0$ . As a result, the rejection rate in the first row of Panel B is fixed at 0.05.

The rejection rates in Panel A of Table 2 indicate that our approach generally yields higher rejection power than the prior in [Chan \(2018\)](#), although the latter performs better for the Markov-switching DGP with the smaller sample size. Overall, both priors identify homoskedasticity of the first shock effectively and show strong performance in rejecting it when the first shock follows either SV or GARCH volatility. Rejection becomes more difficult when the volatility process is Markov-switching. Panel B confirms these results, with both priors delivering very similar rejection rates. Overall, our second MC exercise shows that the homoskedasticity verification method provides a reliable way to assess partial identification through heteroskedasticity. These results further support the use of the method in practice.<sup>4</sup>

---

<sup>4</sup>We acknowledge that several Bayesian and frequentist methods have been proposed for testing identification through heteroskedasticity in structural VARs, including [Lanne and Saikkonen \(2007\)](#), [Lütkepohl and Milunovich \(2016\)](#), [Lewis \(2021\)](#), and [Lütkepohl and Woźniak \(2020\)](#). We ran simulations for all of these methods and report the results in Supplementary Materials. Since their null hypotheses differ from ours, they are not directly comparable. Moreover, some of these methods are tailored to specific volatility models and can perform well in such settings, but none consistently outperforms our approach across all scenarios. Each exhibits clear weaknesses in parts of our simulation design, so none emerges as a generally preferable alternative.

## 6. Empirical application: identifying tax shocks

In this section, we illustrate the usefulness of the non-centred approach for identifying tax shocks. This empirical exercise is estimated using a posterior simulation algorithm, with details provided in Supplementary Materials.

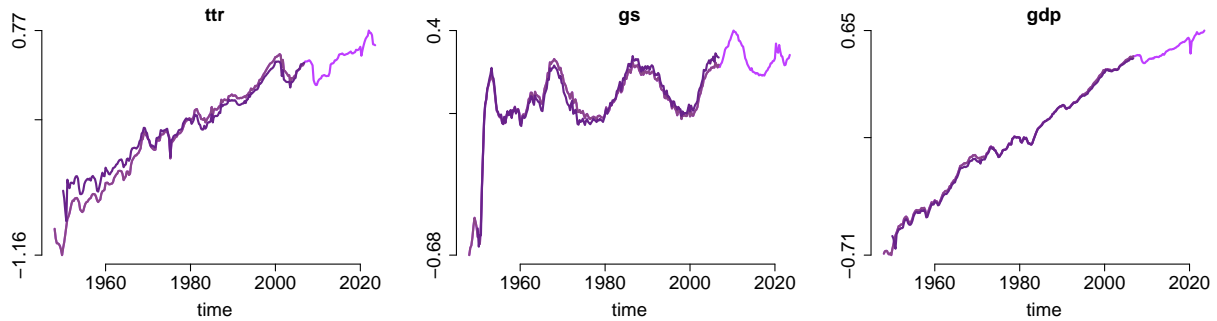
When heteroskedasticity is used for identification in SVAR analysis, the shocks are distinguished by their variances or conditional variances. This approach provides distinct shocks without economic labels and requires some additional information to label the shocks. Such information is sometimes available in the form of specific shapes of the impulse responses associated with a shock or a specific sign pattern of the impact effects of the shocks.

To illustrate the methods developed in the previous sections, we will consider a fiscal SVAR model in which the unanticipated tax shock has been identified in different ways. These alternative identification strategies include, for example, [Blanchard and Perotti \(2002\)](#) (henceforth BP), who use restrictions on the short-run effects of the shocks and the instantaneous interactions of the variables to identify their shocks, and by [Mountford and Uhlig \(2009\)](#) using sign restrictions. Moreover, [Mertens and Ravn \(2014\)](#) (henceforth MR), as revised by [Ramey \(2016\)](#), use an external instrument, a narrative measure of the tax shock proposed by [Romer and Romer \(2010\)](#). Finally, [Lewis \(2021\)](#) (henceforth LE) uses heteroskedasticity and, hence, an approach in that respect similar to ours. We use the MR model as our benchmark to illustrate the use of our methodology for identifying the tax shock through heteroskedasticity, and the narrative measure by [Romer and Romer \(2010\)](#) to ensure a correct labelling of the shocks.

### 6.1. A simple fiscal SVAR

MR specify a three-variable fiscal system including total tax revenue, denoted by  $ttr$ , government spendings,  $gs$ , and gross domestic product,  $gdp$ , and they express all the quarterly variables in real, log, per person terms. We will also consider these three variables and investigate whether the tax shock can be identified by our methodology.

Figure 3: Time series of three variables across three samples used for estimation



Note: The figure plots three series for three samples: the 2023-sample plotted in light pink includes observations from 1948Q1 to 2023Q3 ( $T = 303$ ), the 2006-sample plotted in darker pink is as the 2023-sample but finishes in 2006Q4 ( $T = 236$ ), the MR-sample, plotted in purple, spans the period from 1950Q1 to 2006Q4 ( $T = 228$ ). The plotted series are standardized by subtracting from each series its first observation in 1980.

In order to investigate identification through heteroskedasticity in this fiscal system, we use three alternative samples of different lengths and partly different values even for overlapping periods. They are plotted in Figure 3, where it can be seen that the series are different but similar in overlapping periods. The shortest sample, hereafter MR-sample, uses the data from MR and LE that is downloaded directly from Karel Mertens' website.<sup>5</sup> Following the data construction described by MR, total tax revenue, government spending, and gross domestic product, as well as the GDP deflator are taken from NIPA Tables numbers 3.2, 3.9.5, 1.1.5, and 1.1.9, respectively, provided by the [U.S. Bureau of Economic Analysis \(2024c,d,a,b\)](#), and the population variable is provided by [Francis and Ramey \(2009\)](#). This data spans the period 1950Q1 to 2006Q4.

We extend the sample to the latest available observations in 2023Q3 with modifications in the population variable that is replaced by one matching [Francis and Ramey's \(2009\)](#) definition and provided by the [U.S. Bureau of Labor Statistics \(2024\)](#). Based on these variables we form two samples, both of which contain longer time series than MR and start in 1948Q1. One of these samples, hereafter the 2023-sample, ends in 2023Q3, and the

<sup>5</sup>The spreadsheet is available at [https://karelmertenscom.files.wordpress.com/2017/09/jme2014\\_data.xls](https://karelmertenscom.files.wordpress.com/2017/09/jme2014_data.xls)

other one, hereafter the 2006-sample, ends in 2006Q4. Following MR, we use a VAR(4) model with a constant term, a linear and a quadratic trend, and a dummy for 1975Q2 as deterministic terms.

## 6.2. Verifying partial identification through heteroskedasticity

We base our structural analysis on model (2.2). Hence, we have to sample from the posterior of the structural  $\mathbf{B}_0$  matrix, which is not identified without further restrictions if the shocks are homoskedastic. Even if the shocks are identified, the row ordering and row signs may change in different drawings from the posterior if one does not take special precautions to prevent that from happening. We, therefore, follow LE and reorder the rows and adjust their signs such that each draw has the minimum distance to the benchmark  $\mathbf{B}_0$  matrix as in BP. More details on this procedure are provided in Supplementary Materials.<sup>6</sup> Hence, the shocks can be labeled along the lines of BP as an unanticipated tax shock ( $w_t^{tr}$ ), a government spending shock ( $w_t^{gs}$ ), and an additional shock ( $w_t^{gdp}$ ) capturing unexpected changes in  $gdp_t$  not caused by tax or spending shocks. We will label our shocks accordingly although it is, of course, not clear from the outset if the shocks can be identified through heteroskedasticity with our methodology. If they can, they may still differ from those in BP and MR, in which case our labels may not be meaningful. We will return to this issue later.

We next assess whether the labeled shocks are identified through heteroskedasticity. Our main tool for that purpose is the SDDR from Equation (4.1). The SDDR values computed for each of the three shocks individually using our three data samples are reported in Table 3. For the 2023-sample, the evidence for heteroskedasticity of all three structural shocks is strong according to the scale proposed by Kass and Raftery (1995). The values of the log Bayes factors shown in Table 3 indicate that the posterior mass in favour of heteroskedasticity exceeds 99% for all the shocks. This result provides strong evidence for the identification of all three shocks through heteroskedasticity in the 2023-sample and

---

<sup>6</sup>We also experiment with alternative benchmark estimates for  $\mathbf{B}_0$ . The results are virtually unchanged and are reported in Supplementary Materials.

Table 3: Verification of partial identification of structural shocks through heteroskedasticity across samples

Structural shocks	2023-sample	2006-sample	MR-sample
$w_t^{tr}$	<b>-21.38</b> [4.69]	-1.51 [0.18]	0.32 [0.05]
$w_t^{ss}$	<b>-4.62</b> [0.79]	-1.32 [0.15]	0.23 [0.05]
$w_t^{gdp}$	<b>-63.39</b> [6.43]	0.50 [0.03]	0.39 [0.03]

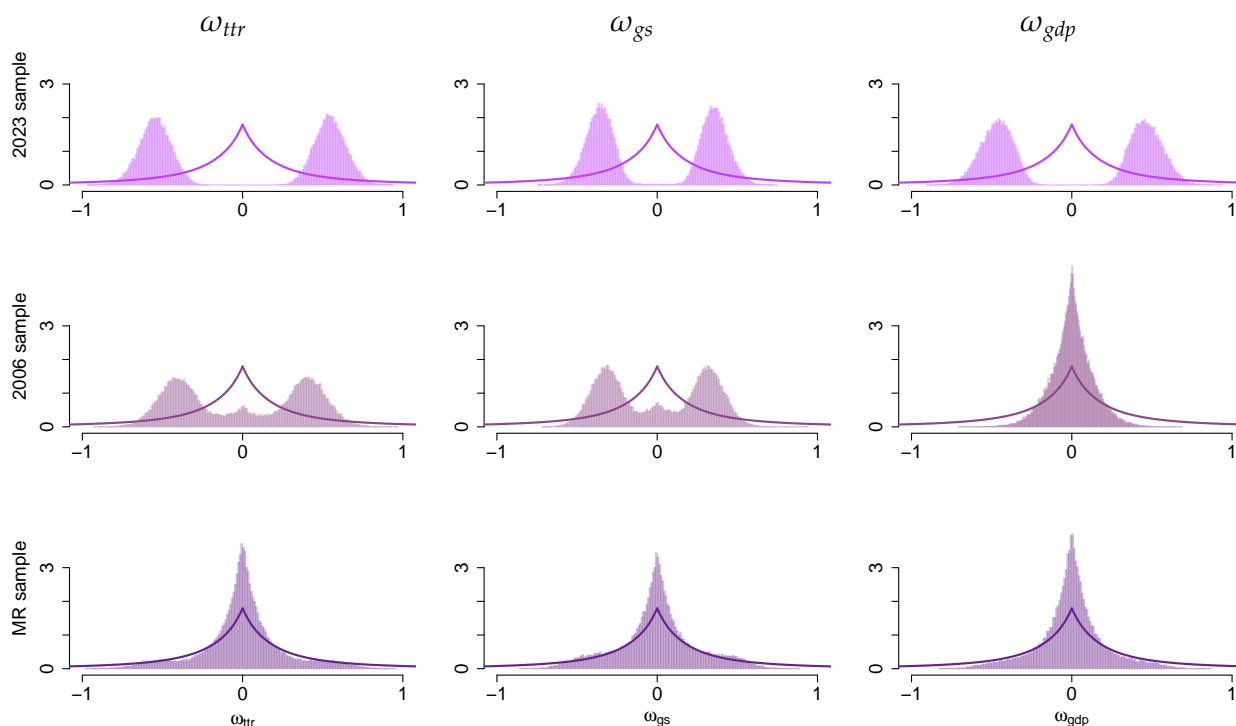
Note: The table reports the log of the Bayes factors estimated via the log of SDDRs from Equation (4.1) together with numerical standard errors (NSEs) provided in brackets. Negative values provide evidence against homoskedasticity. Bold font numbers represent cases in which the evidence for heteroskedasticity is positive (values greater than 3 in absolute terms) or strong (greater than 20) on the scale of [Kass and Raftery \(1995\)](#). The NSEs are computed based on 30 subsamples of the original MCMC draws.

is robust to many variations in the model prior specification. These variations include perturbations of the hyper-parameters that need to be fixed in our setup. We checked the conclusions for three values of each scale and shape of the prior distribution for  $\omega_n$ , as well as for three alternative setups for the hyper-parameters for each of the matrices  $\mathbf{A}_i$  and  $\mathbf{B}_0$ . Each of these alternative setups included cases of stronger and weaker shrinkage than in our benchmark prior specification.

The evidence for the structural shocks to be identified through heteroskedasticity is much weaker in the 2006-sample. Moreover, the log Bayes factors estimated by the log-SDDRs for the MR-sample are positive, implying that the posterior mass for homoskedasticity is greater than that for heteroskedasticity. The log-SDDRs are negative for the last two shocks in the 2006-sample, which includes eight more observations than the MR-sample from the volatile late 1940s. More specifically, in the 2006-sample, the posterior probability of the heteroskedastic shock  $w_t^{tr}$  is 82%. Obviously, in this case, the evidence for identification through heteroskedasticity of the first shock is limited and it is even more limited for the other shocks. These findings are also robust to the perturbations in the values of the prior hyper-parameters.

In Figure 4, we further illustrate how the SDDRs work by plotting the marginal prior versus the marginal posterior densities of  $\omega_n$  associated with our three samples. Based

Figure 4: Marginal prior (solid line) and posterior (histograms) densities of  $\omega_{ttr}$ ,  $\omega_{gs}$ , and  $\omega_{gdp}$  across samples



Note: The marginal prior density is estimated by numerical integration as in [Gelfand and Smith \(1990\)](#) using a grid of points from -1.1 to 1.1. They are the same for all samples and shocks. The marginal posterior densities are approximated using histograms. The ratio of these densities at point zero approximates the SDDR in Equation (4.1). Posterior mass less concentrated than the prior mass about zero provides evidence against homoskedasticity.

on the information from these plots, the SDDRs from Equation (4.1) can be approximated by the ratio of the marginal posterior ordinate at zero to that of the marginal prior density. The figures for the 2023-sample exhibit posterior mass concentrated away from the origin and the bi-modality discussed in Section 2, providing evidence against homoskedasticity. Instead, the posterior mass for the 2006- and MR-samples is concentrated about the hypothesis of homoskedasticity, often more than the prior, thus favouring homoskedasticity.

Finally, we analyze the sequences of conditional variances of the structural shocks that are required to be clearly distinct for partial identification of the shocks to hold according

to Theorem A.1. We plot their posterior means together with 90% highest posterior density (HPD) intervals in Figure 5.<sup>7</sup> The conditional variances are visibly time varying for the 2023-sample. The conditional variances of the first shock are significantly different from 1 in six periods in that sample, including the mid-70s and mid-80s, individual quarters in 2001, 2002, and 2003, and the first quarter of 2009. The variances of the second shock are different from 1 in the first quarter of 1951 only, while those of the third shock have HPD intervals not including 1 in 1950 and quarters 2 and 3 of 2020. The distinctive occurrence times of high volatility periods for the three shocks provide strong evidence for them to be different in these sequences, further supporting the identification through heteroskedasticity in this sample. In particular, this evidence supports our claim that the first shock is identified as its conditional variances evolve non-proportionally to those of other shocks.

The conditional variances in the 2006-sample are to some extent similar to those from the 2023-sample until 2006. However, at all times, the 90% HPD intervals include the value of 1. This is caused by a weaker signal provided from the data in the shorter sample regarding time-varying volatility, which undermines the evidence for identification in the framework of our model. In the MR-sample, the evidence for conditional variances that support identification is even weaker. Thus, the bottom line is that, in the 2023-sample, the shocks are clearly identified through heteroskedasticity, while the evidence for identification through heteroskedasticity is weaker in the 2006-sample, and no such evidence is found in the MR-sample.

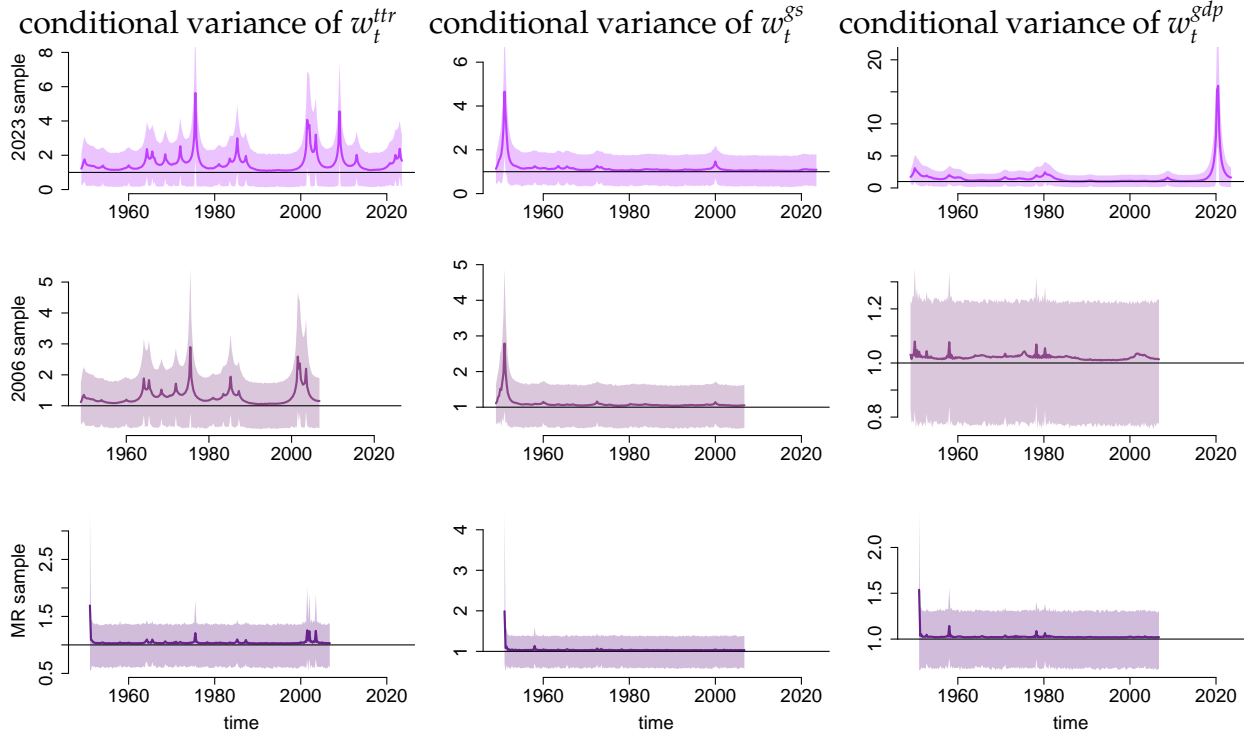
### *6.3. The effects of tax shocks*

Thus far, we document varying degrees of evidence of partial identification of structural shocks across samples. The MR-sample shows no evidence and is therefore excluded from further analysis. Given that heteroskedasticity provides three identified shocks for the 2023-sample, we examine which one corresponds to the tax shock. To do so, we begin

---

<sup>7</sup>See Supplementary Materials for the centred parameterization version of these time-varying conditional variances.

Figure 5: Conditional variance of structural shocks across samples



Note: The figures plot time-varying conditional variances of the structural shocks. The lines report the posterior mean and the shaded areas 90% HPD intervals. The variances in the first row clearly exhibit non-proportional changes across time. The horizontal black line is set at the value of 1, around which the prior is centred.

by reporting the correlations between the structural shocks from our estimated model and the narrative measure of an unanticipated tax shock by [Romer and Romer \(2010\)](#), based on the 2006- and 2023-samples. These correlations are presented in [Table 4](#).

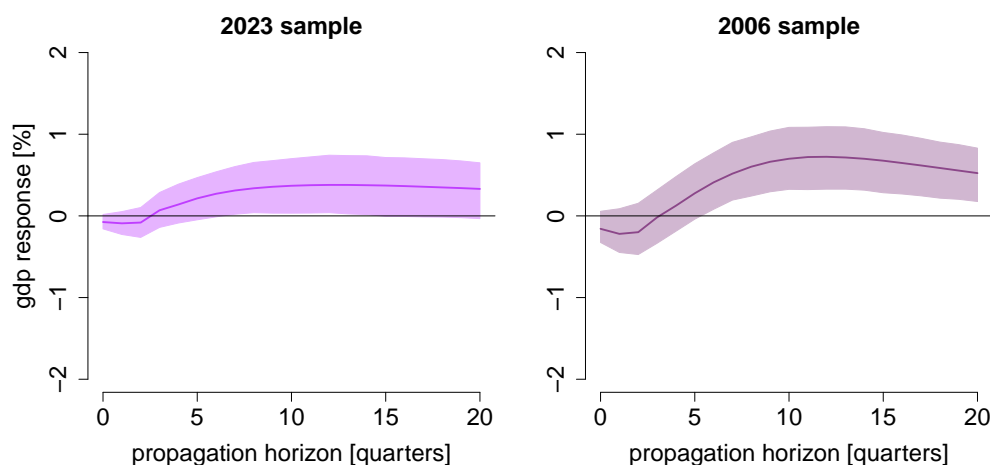
The results show that the first shock in our models is, albeit modestly, the most correlated with the narrative measure of [Romer and Romer \(2010\)](#). Such low correlations are consistent with the *weak instrument* observation of [Ramey \(2016\)](#), yet exceed 0.22 for all models in [Table 4](#). They are also higher than those for the second shock, with values of -0.022 for the 2023-sample and 0.03 for the 2006-sample, and for the third shock, which reports correlations below -0.15 in both samples. Notably, the correlations for the first shock are similar to those of the tax shocks estimated by BP, MR, and LE, reported in

Table 4: Correlations between the narrative tax shock measure of [Romer and Romer \(2010\)](#) and the three structural shocks in our model, as well as with other tax shocks proposed in the literature

Structural shocks	2023-sample	2006-sample	BP results	MR results	LE results
$w_t^{ttr}$	0.224	0.264	0.277	0.298	0.233
$w_t^{gs}$	-0.022	0.030			
$w_t^{gdp}$	-0.154	-0.170			

Note: The table reports sample correlations between the narrative measure of tax shocks proposed by [Romer and Romer \(2010\)](#) and used by MR. The results in the 2023-sample and 2006-sample columns are based on our posterior estimations, where we used the posterior mean of the shocks as their estimator. The results in the BP results, MR results, and LE results columns are based on our reproduction of the results from MR and LE using the authors' computer codes and data.

Figure 6: Impulse responses of gross domestic product to a negative tax shock: our estimates

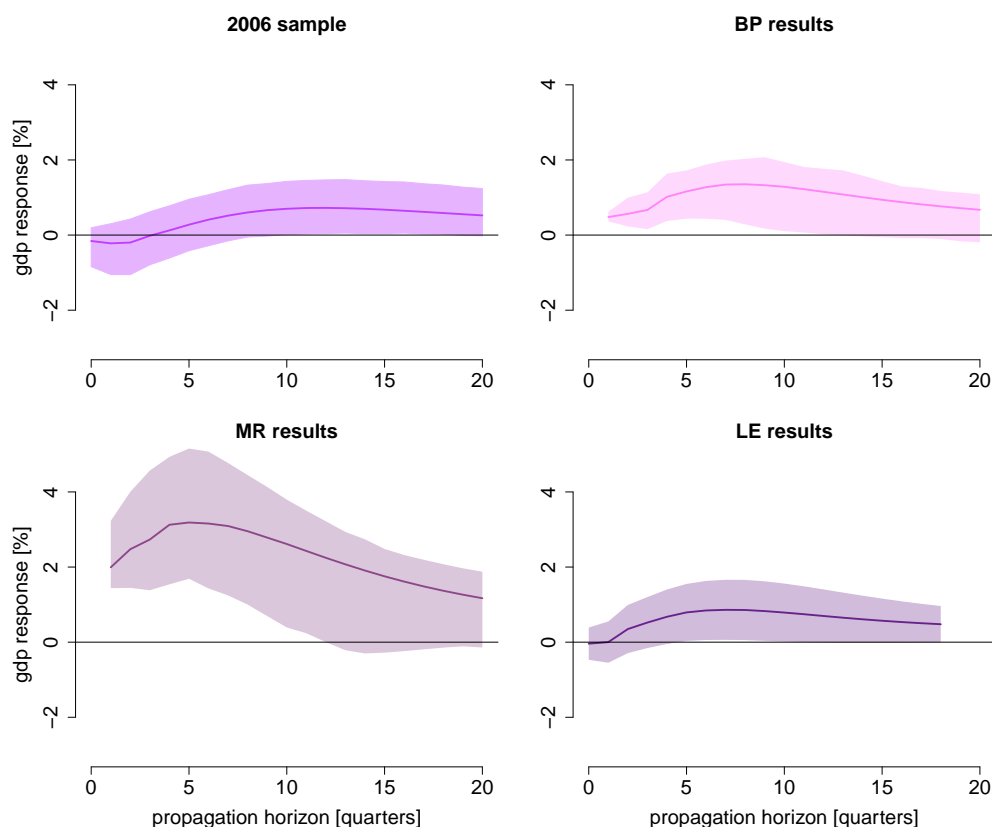


Note: The figure reports impulse responses of  $gdp_t$  to a negative tax shock lowering  $ttr_t$  by 1% of the  $gdp_t$  value in the last quarter of 2006. The lines report the posterior medians and the shaded areas the 68% HPD point-wise intervals.

the last three columns of Table 4. Taken together, this correlation analysis provides some support for interpreting the first shock as the *tax shock*.

Next, we investigate the dynamic effects of the tax shock identified with our approach on  $gdp_t$ . Figure 6 reports the corresponding impulse responses for both the 2006- and 2023-samples. Following MR and LE, these responses correspond to a tax shock that

Figure 7: Impulse responses of gross domestic product to a negative tax shock: comparison with other studies



Note: The figure reports impulse responses of  $gdp_t$  to a negative tax shock lowering  $ttr_t$  by 1% of the  $gdp_t$  value in the last quarter of 2006. In the 2006-sample plot, the line reports the posterior median and the shaded area reports the 90% HPD point-wise interval for the PM-ordering. In the remaining plots, the lines report the maximum likelihood estimator and the shaded areas, the 95% point-wise confidence intervals.

reduces  $ttr_t$  by 1% of  $gdp_t$ . The impulse responses in Figure 6 share two common features: (i) no effect on impact and during the first six quarters, and (ii) a subsequent increase in  $gdp_t$ , reaching a peak thirteen quarters after the shock at about 0.38% for the 2023-sample and 0.73% for the 2006-sample. The shorter-sample shock is more persistent, with effects that remain significant even five years after impact, whereas in the longer sample the response dies out after roughly 3.5 years. Overall, the shapes of the impulse responses from the 2023- and 2006-samples are quite similar.

We also examine how the impulse response based on our 2006-sample compares with those reported in BP, MR, and LE for the MR-sample, i.e., the original data used by these authors.<sup>8</sup> Figure 7 presents these results with the 90% HDP intervals for our model estimates. The impulse responses in BP, MR, and LE are maximum likelihood estimates with 95% confidence intervals.

Our results share two features with those in the literature: the peak occurs at mid-horizons, and statistical significance fades after three to four years. In addition, our peak response is close to those in BP and LE, whereas MR obtain a larger peak. A further difference is that only the impulse responses reported by LE are statistically insignificant on impact and in the following four quarters—as in our estimates—while BP and MR report positive and significant responses on impact. Overall, however, the conclusions from our estimates remain broadly consistent with the literature, even though they are obtained using a different identification approach, namely identification through non-centred stochastic volatility.

## 7. Conclusion

This paper studied how structural shocks can be identified in SVAR-SVs under Bayesian estimation, with a focus on the role of the non-centred parameterization for stochastic volatility. Our results highlight three main contributions.

First, we show that the non-centred parameterization leads to a marginal prior on the conditional variances of shocks that, unlike the common centred parameterization, is centred at homoskedasticity, with shrinkage and heavy tails. At the same time, the implied prior structure is consistent with the view—emphasized in earlier work on volatility comovement—that widespread heteroskedasticity in macroeconomic and financial series can often be traced back to a limited number of underlying shocks. In this sense, the non-centred parameterization not only facilitates partial identification, but also aligns the modeling framework with empirical evidence on the sources of volatility. As a byproduct

---

<sup>8</sup>Our BP results rely on the SVAR model of [Blanchard and Perotti \(2002\)](#), as estimated by [Mertens and Ravn \(2014\)](#).

of our main theoretical contribution, we also establish that the conditions for partial identification can be verified in practice. In particular, we derive the requirements under which such a verification procedure is feasible, and show how it can be implemented using the SDDR approach.

Second, our MC experiments demonstrate that adopting the non-centered parameterization yields systematic gains in estimation accuracy. Most notably, the parameters central to shock identification—the conditional variances and the corresponding rows of the impact matrix—exhibit consistently lower estimation error, with improvements in both small and large systems.

Third, applying our framework to well-known tax SVARs, we show that the non-centred approach can successfully identify tax shocks through heteroskedasticity. The resulting shocks align closely with estimates reported in the literature, indicating that the method is not only theoretically appealing but also reliable in applied settings.

Overall, the non-centred parameterization provides a simple but powerful way to exploit identification through stochastic volatility in SVARs. Although our analysis has focused on a fiscal application, the approach is easily adaptable to other areas of macroeconomics and finance where identification is partial or uncertain. An interesting avenue for future research is to examine its performance in more flexible settings, such as in [Camehl and Woźniak \(2024\)](#), where both the volatility of structural shocks and the impact matrix are allowed to vary over time.

## **8. Acknowledgments**

For their useful comments and suggestions, we would like to thank Professor Subal Kumbhakar and Professor Sushanta Mallick (Editors), an anonymous Associate Editor, two anonymous referees, as well as participants at various seminars and conferences. This research did not receive any specific grant from funding agencies in the public, commercial, or not-for-profit sectors.

## References

- Barndorff-Nielsen, O. E. (1997). Normal inverse gaussian distributions and stochastic volatility modelling. *Scandinavian Journal of Statistics* 24(1), 1–13.
- Baumeister, C. and G. Peersman (2013, October). Time-varying effects of oil supply shocks on the us economy. *American Economic Journal: Macroeconomics* 5(4), 1–28.
- Belmonte, M. A., G. Koop, and D. Korobilis (2014). Hierarchical Shrinkage in Time-Varying Parameter Models: Hierarchical Shrinkage in Time-Varying Parameter Models. *Journal of Forecasting* 33(1), 80–94.
- Benjamini, Y. and Y. Hochberg (1995). Controlling the false discovery rate: A practical and powerful approach to multiple testing. *Journal of the Royal Statistical Society: Series B (Methodological)* 57(1), 289–300.
- Bertsche, D. and R. Braun (2022). Identification of Structural Vector Autoregressions by Stochastic Volatility. *Journal of Business & Economic Statistics* 40(1), 328–341.
- Bitto, A. and S. Frühwirth-Schnatter (2019). Achieving shrinkage in a time-varying parameter model framework. *Journal of Econometrics* 210(1), 75–97.
- Blanchard, O. and R. Perotti (2002, November). An Empirical Characterization of the Dynamic Effects of Changes in Government Spending and Taxes on Output. *The Quarterly Journal of Economics* 117(4), 1329–1368.
- Cadonna, A., S. Frühwirth-Schnatter, and P. Knaus (2020). Triple the gamma unifying shrinkage prior for variance and variable selection in sparse state space and tvp models. *Econometrics* 8(2), 20.
- Camehl, A. and T. Woźniak (2024). Time-varying identification of monetary policy shocks. *arXiv preprint arXiv:2311.05883*.
- Carriero, A., T. E. Clark, and M. Marcellino (2016, July). Common drifting volatility in large bayesian vars. *Journal of Business & Economic Statistics* 34(3), 375–390.
- Castelnuovo, E., K. Tuzcuoglu, and L. Uzeda (2025, March). Sectoral uncertainty: A hierarchical-volatility approach. *Journal of Business & Economic Statistics* 43(1), 1–13.
- Chan, J. C. C. (2018). Specification tests for time-varying parameter models with stochastic volatility. *Econometric Reviews* 37(8), 807–823.
- Chan, J. C. C., G. Koop, and X. Yu (2024). Large order-invariant bayesian vars with stochastic volatility. *Journal of Business & Economic Statistics* 42(2), 825–837.
- Clark, T. E. (2011). Real-time Density Forecasts from Bayesian Vector Autoregressions with Stochastic Volatility. *Journal of Business and Economic Statistics* 29(3), 327–341.
- Clark, T. E. and F. Ravazzolo (2015). Macroeconomic Forecasting Performance Under Alternative Specification of Time-Varying Volatility. *Journal of Applied Econometrics* 30, 551–575.
- Cogley, T. and T. J. Sargent (2005). Drifts and Volatilities: Monetary Policies and Outcomes in the Post WWII US. *Review of Economic Dynamics* 8, 262–302.

- Engel, C. and S. Kozicki (1992, July). Testing for common features. *Journal of Business & Economic Statistics* 10(3), 317–327.
- Francis, N. and V. A. Ramey (2009). Measures of per capita hours and their implications for the technology-hours debate. *Journal of Money, Credit and Banking* 41(6), 1071–1097.
- Frühwirth-Schnatter, S. and H. Wagner (2010, January). Stochastic model specification search for gaussian and partial non-gaussian state space models. *Journal of Econometrics* 154(1), 85–100.
- Gelfand, A. E. and A. F. M. Smith (1990, jun). Sampling-Based Approaches to Calculating Marginal Densities. *Journal of the American Statistical Association* 85(410), 398–409.
- Herwartz, H. and H. Lütkepohl (2014). Structural vector autoregressions with Markov switching: Combining conventional with statistical identification of shocks. *Journal of Econometrics* 183, 104–116.
- Kass, R. E. and A. E. Raftery (1995). Bayes Factors. *Journal of the American Statistical Association* 90(430), 773–795.
- Kastner, G. and S. Frühwirth-Schnatter (2014). Ancillarity-sufficiency interweaving strategy (asis) for boosting mcmc estimation of stochastic volatility models. *Computational Statistics & Data Analysis* 76, 408–423.
- Kilian, L. and H. Lütkepohl (2017). *Structural Vector Autoregressive Analysis*. Cambridge: Cambridge University Press.
- Lanne, M. and J. Luoto (2021, January). Gmm estimation of non-gaussian structural vector autoregression. *Journal of Business & Economic Statistics* 39(1), 69–81.
- Lanne, M. and H. Lütkepohl (2008). Identifying monetary policy shocks via changes in volatility. *Journal of Money, Credit and Banking* 40, 1131–1149.
- Lanne, M., H. Lütkepohl, and K. Maciejowska (2010). Structural vector autoregressions with Markov switching. *Journal of Economic Dynamics and Control* 34, 121–131.
- Lanne, M. and P. Saikkonen (2007). A multivariate generalized orthogonal factor garch model. *Journal of Business & Economic Statistics* 25(1), 61–75.
- Lewis, D. J. (2021). Identifying Shocks via Time-Varying Volatility. *The Review of Economic Studies* 88(6), 3086–3124.
- Lütkepohl, H., M. Meitz, A. Netšunajev, and P. Saikkonen (2021). Testing identification via heteroskedasticity in structural vector autoregressive models. *The Econometrics Journal* 24(1), 1–22.
- Lütkepohl, H. and A. Netšunajev (2017). Structural vector autoregressions with smooth transition in variances. *Journal of Economic Dynamics and Control* 84, 43–57.
- Lütkepohl, H. and A. Velinov (2016). Structural vector autoregressions: Checking identifying long-run restrictions via heteroskedasticity. *Journal of Economic Surveys* 30, 377–392.
- Lütkepohl, H. and T. Woźniak (2020). Bayesian inference for structural vector autoregressions identified by

- Markov-switching heteroskedasticity. *Journal of Economic Dynamics and Control* 113, 103862.
- Lütkepohl, H. and G. Milunovich (2016). Testing for identification in SVAR-GARCH models. *Journal of Economic Dynamics and Control* 73, 241–258.
- Mertens, K. and M. O. Ravn (2014). A reconciliation of SVAR and narrative estimates of tax multipliers. *Journal of Monetary Economics* 68, S1–S19.
- Mountford, A. and H. Uhlig (2009). What are the effects of fiscal policy shocks? *Journal of Applied Econometrics* 24(6), 960–992.
- Netšunajev, A. (2013). Reaction to technology shocks in Markov-switching structural VARs: Identification via heteroskedasticity. *Journal of Macroeconomics* 36, 51–62.
- Omori, Y., S. Chib, N. Shephard, and J. Nakajima (2007). Stochastic Volatility with Leverage: Fast and Efficient Likelihood Inference. *Journal of Econometrics* 140(2), 425–449.
- Primiceri, G. E. (2005, July). Time varying structural vector autoregressions and monetary policy. *The Review of Economic Studies* 72(3), 821–852.
- Ramey, V. A. (2016). Macroeconomic shocks and their propagation. *Handbook of Macroeconomics* 2, 71–162.
- Rigobon, R. (2003). Identification through heteroskedasticity. *Review of Economics and Statistics* 85, 777–792.
- Rigobon, R. and B. Sack (2003). Measuring the reaction of monetary policy to the stock market. *Quarterly Journal of Economics* 118, 639–669.
- Romer, C. D. and D. H. Romer (2004). A new measure of monetary shocks: Derivation and implications. *American Economic Review* 94(4), 1055–1084.
- Romer, C. D. and D. H. Romer (2010). The Macroeconomic Effects of Tax Changes: Estimates Based on a New Measure of Fiscal Shocks. *American Economic Review* 100(3), 763–801.
- Rubio-Ramírez, J. F., D. F. Waggoner, and T. Zha (2010). Structural Vector Autoregressions: Theory of Identification and Algorithms for Inference. *Review of Economic Studies* 77(2), 665–696.
- Sentana, E. and G. Fiorentini (2001). Identification, estimation and testing of conditionally heteroskedastic factor models. *Journal of Econometrics* 102, 143–164.
- Stock, J. H. and M. W. Watson (2007, February). Why has u.s. inflation become harder to forecast? *Journal of Money, Credit and Banking* 39(Supp. 1), 3–33. Special issue on inflation forecasting.
- Storey, J. D. (2002). A direct approach to false discovery rates. *Journal of the Royal Statistical Society: Series B (Statistical Methodology)* 64(3), 479–498.
- U.S. Bureau of Economic Analysis (2024a). Table 1.1.5. Gross Domestic Product. Data. Retrieved from NIPA Tables [accessed January 2, 2024].
- U.S. Bureau of Economic Analysis (2024b). Table 1.1.9. Implicit Price Deflators for Gross Domestic Product. Data. Retrieved from NIPA Tables [accessed January 2, 2024].
- U.S. Bureau of Economic Analysis (2024c). Table 3.2. Federal Government Current Receipts and

- Expenditures. Data. Retrieved from NIPA Tables [accessed January 2, 2024].
- U.S. Bureau of Economic Analysis (2024d). Table 3.9.5. Government Consumption Expenditures and Gross Investment. Data. Retrieved from NIPA Tables [accessed January 2, 2024].
- U.S. Bureau of Labor Statistics (2024). Population Level [CNP16OV]. Data, Federal Reserve Bank of St. Louis. Retrieved from FRED Database [accessed January 2, 2024].
- Uzeda, L. (2022). State correlation and forecasting: A bayesian approach using unobserved components models. In *Essays in Honour of Fabio Canova*, Volume 44 of *Advances in Econometrics*, pp. 25–53. Emerald Group Publishing Limited. Published 2023.
- Waggoner, D. F. and T. Zha (2003a). A Gibbs Sampler for Structural Vector Autoregressions. *Journal of Economic Dynamics & Control* 28(2), 349–366.
- Waggoner, D. F. and T. Zha (2003b, June). Likelihood preserving normalization in multiple equation models. *Journal of Econometrics* 114(2), 329–347.
- Woźniak, T. (2024). *bsvars: Bayesian Estimation of Structural Vector Autoregressive Models*. R package version 3.2.
- Woźniak, T. (2025). Fast and Efficient Bayesian Analysis of Structural Vector Autoregressions Using the R Package bsvars. Working paper, University of Melbourne.
- Woźniak, T. and M. Droumaguet (2015). Assessing Monetary Policy Models: Bayesian Inference for Heteroskedastic Structural VARs. *University of Melbourne Working Papers Series* 2017.

## A. Partial identification in heteroskedastic SVARs: Theorem A.1 and proofs

The following matrix result is the basis for partial identification of structural parameters in structural VAR models with general heteroskedastic or conditionally heteroskedastic structural shocks.

**Theorem A.1.** Let  $\Sigma_t$ ,  $t = 0, 1, \dots$ , be a sequence of positive definite  $N \times N$  matrices and  $\Lambda_t = \text{diag}(\sigma_{1,t}^2, \dots, \sigma_{N,t}^2)$  a sequence of  $N \times N$  diagonal matrices with  $\Lambda_0 = \mathbf{I}_N$ . Suppose there exists a nonsingular  $N \times N$  matrix  $\mathbf{B}_0$  such that

$$\Sigma_t = \mathbf{B}_0^{-1} \Lambda_t \mathbf{B}_0^{-1'}, \quad t = 0, 1, \dots \quad (\text{A.1})$$

Let  $\sigma_n^2 = (1, \sigma_{n,1}^2, \sigma_{n,2}^2, \dots)$  be a possibly infinite dimensional vector. Then the  $n^{\text{th}}$  row of  $\mathbf{B}_0$  is unique up to sign if  $\sigma_n^2 \neq \sigma_i^2 \quad \forall i \in \{1, \dots, N\} \setminus \{n\}$ .

Assuming that the  $\Sigma_t$  are the covariance matrices of the reduced-form residuals in a VAR model and the  $\Lambda_t$  are the covariance matrices of the structural shocks, the theorem generalizes Theorem 1 of [Lütkepohl and Woźniak \(2020\)](#) which presents an analogous result for structural errors with volatility changes generated by a homogeneous Markov switching process with finitely many volatility states. Our Theorem A.1 provides a general result on identification of a single equation through heteroskedasticity and also applies, for instance, if the volatility changes are generated by a different Markov process for each shock. It shows that a structural shock and, hence, the corresponding structural equation is identified if the sequence of variances is distinct from the variance sequences of any of the other shocks. Our Theorem A.1 generalizes identification results for some special volatility models that have been used in the literature on identification through heteroskedasticity (see, e.g., [Kilian and Lütkepohl, 2017](#), Chapter 14). For example, it is easy to see that identification results for volatility models based on a finite number of volatility regimes as considered by [Rigobon \(2003\)](#), [Rigobon and Sack \(2003\)](#), [Lanne and Lütkepohl \(2008\)](#), [Lanne, Lütkepohl, and Maciejowska \(2010\)](#), [Netšunajev \(2013\)](#), [Herwartz and Lütkepohl \(2014\)](#), [Woźniak and Droumaguet \(2015\)](#), [Lütkepohl and Velinov \(2016\)](#), [Lütkepohl and Netšunajev \(2017\)](#) follow directly from Theorem A.1.

We emphasize that Theorem A.1 also implies identification conditions for the SV models considered in this study. In this context, SV models have also been proposed by [Lewis \(2021\)](#) and [Bertsche and Braun \(2022\)](#). In such cases, the conditional covariance matrices of the reduced form errors are given by  $\Sigma_t = \mathbf{B}_0^{-1} \Lambda_t \mathbf{B}_0^{-1'}$ , where  $\Lambda_t = \text{diag}(\sigma_{1,t}^2, \dots, \sigma_{N,t}^2)$  is a diagonal matrix. If the  $\sigma_{n,t}^2$  vary stochastically, as in SV dynamics, they will not be proportional with probability 1 and, hence, satisfy the conditions for identification of Theorem A.1. So if any one of the structural errors has changing conditional variances, it will be identified, even if all the other components have constant conditional variance. That insight is used in our Bayesian analysis of the SV model. It may be worth noting, however, that Theorem A.1 also implies that a single shock may be homoskedastic and still be identified in case all other shocks are heteroskedastic. This discussion also shows that Theorem A.1 generalizes results for full

identification in [Sentana and Fiorentini \(2001\)](#), [Lewis \(2021\)](#), and [Bertsche and Braun \(2022\)](#) to the case of partial identification.

*Proof of Theorem A.1*

We first prove the following lemma.

**Lemma A.1.** *Let  $\Sigma_t$ ,  $t = 0, 1, \dots$ , be a sequence of positive definite  $N \times N$  matrices and  $\Lambda_t = \text{diag}(\sigma_{1,t}^2, \dots, \sigma_{N,t}^2)$  a sequence of  $N \times N$  diagonal matrices with  $\Lambda_0 = \mathbf{I}_N$ . Suppose there exists a nonsingular  $N \times N$  matrix  $\mathbf{B}$  such that*

$$\Sigma_t = \mathbf{B}\Lambda_t\mathbf{B}', \quad t = 0, 1, \dots \quad (\text{A.2})$$

*Let  $\sigma_n^2 = (1, \sigma_{n,1}^2, \sigma_{n,2}^2, \dots)$  be a possibly infinite dimensional vector. Then the  $n^{\text{th}}$  column of  $\mathbf{B}$  is unique up to sign if  $\sigma_n^2 \neq \sigma_i^2 \quad \forall i \in \{1, \dots, N\} \setminus \{n\}$ .*

*Proof.* Let  $\mathbf{B}_*$  be a matrix that satisfies:  $\Sigma_t = \mathbf{B}_*\Lambda_t\mathbf{B}_*'$ ,  $t = 0, 1, \dots$ . It will be shown that, under the conditions of Lemma A.1, the  $n^{\text{th}}$  column of  $\mathbf{B}_*$  must be the same as that of  $\mathbf{B}$ , except perhaps for a reversal of signs. Without loss of generality, it is assumed in the following that  $n = 1$  because this simplifies the notation. In other words, it is shown that the first columns of  $\mathbf{B}$  and  $\mathbf{B}_*$  are the same except for a reversal of signs if  $\sigma_1^2 \neq \sigma_i^2$ ,  $i = 2, \dots, N$ .

There exists a nonsingular  $N \times N$  matrix  $\mathbf{Q}$  such that  $\mathbf{B}_* = \mathbf{B}\mathbf{Q}$ . Using  $\Sigma_0 = \mathbf{B}\mathbf{B}'$ ,  $\mathbf{Q}$  has to satisfy the relation

$$\mathbf{B}\mathbf{B}' = \mathbf{B}\mathbf{Q}\mathbf{Q}'\mathbf{B}'.$$

Multiplying this relation from the left by  $\mathbf{B}^{-1}$  and from the right by  $\mathbf{B}^{-1'}$  implies that  $\mathbf{Q}\mathbf{Q}' = \mathbf{I}_N$  and, hence,  $\mathbf{Q}$  is an orthogonal matrix.

The relations

$$\mathbf{B}\Lambda_t\mathbf{B}' = \mathbf{B}\mathbf{Q}\Lambda_t\mathbf{Q}'\mathbf{B}'$$

imply  $\Lambda_t = \mathbf{Q}\Lambda_t\mathbf{Q}'$  and, hence,  $\mathbf{Q}\Lambda_t = \Lambda_t\mathbf{Q}$  for all  $t = 0, 1, \dots$

Denoting the  $(i,j)$ <sup>th</sup> element of  $\mathbf{Q}$  by  $q_{ij}$ , the latter equation implies that

$$q_{n1}\sigma_1^2 = q_{n1}\sigma_n^2, \quad n = 1, \dots, N.$$

Hence, since  $\sigma_n^2$  is different from  $\sigma_1^2$  for  $n = 2, \dots, N$ , we must have  $q_{n1} = 0$  for  $n = 2, \dots, N$ . Since,  $\mathbf{Q}$  is orthogonal, the first column must then be

$$(1, 0, \dots, 0)' \quad \text{or} \quad (-1, 0, \dots, 0)'$$

which proves the lemma. □

Now consider the setup of Theorem A.1 with  $\mathbf{B} = \mathbf{B}_0^{-1}$ . Then the arguments in the proof of Lemma A.1 show that  $\mathbf{B}_{0*}^{-1} = \mathbf{B}_0^{-1}\mathbf{Q}$ , where  $\mathbf{Q}$  is as in the proof of Lemma A.1. Hence,  $\mathbf{B}_{0*} = \mathbf{Q}'\mathbf{B}_0$ , which shows that  $\mathbf{B}_{0*}$  and  $\mathbf{B}_0$  have the same  $n^{\text{th}}$  row up to sign. □

Theorem A.1 implies that, if a structural shock is identified, the corresponding structural impulse responses are unique. This result is stated formally in the following corollary.

**Corollary A.1.** *Under the conditions of Theorem A.1, if the  $n^{\text{th}}$  row of  $\mathbf{B}_0$  is unique, then for a given sequence of  $N \times N$  matrices  $\Phi_i$ ,  $i = 0, 1, \dots$ , the  $n^{\text{th}}$  column of the matrix  $\Theta_i = \Phi_i\mathbf{B}_0^{-1}$ , is unique for  $i = 0, 1, \dots$*

*Proof.* It has to be shown that uniqueness of the  $n^{\text{th}}$  row of  $\mathbf{B}_0$  implies a unique  $n^{\text{th}}$  column of  $\mathbf{B}_0^{-1}$ . Without loss of generality we focus on the first row. If the first row of  $\mathbf{B}_0$  is unique, any other admissible  $\mathbf{B}_0$  matrix must be of the form  $\mathbf{Q}\mathbf{B}_0$ , where  $\mathbf{Q}$  is an orthogonal matrix of the form:

$$\begin{bmatrix} 1 & \mathbf{0}_{(1 \times (N-1))} \\ \mathbf{0}_{((N-1) \times 1)} & \mathbf{Q}_* \end{bmatrix},$$

with  $\mathbf{Q}_*$  being an orthogonal  $(N-1) \times (N-1)$  matrix. This fact follows from the arguments in the proof of Lemma A.1. Thus, any admissible inverse has the form  $\mathbf{B}_0^{-1}\mathbf{Q}'$  and, hence,

has the same first column as  $\mathbf{B}_0^{-1}$ . Clearly, the same argument applies for any other row of  $\mathbf{B}_0$ . □

# Supplementary Materials: Partial Identification of Structural Vector Autoregressions with Non-Centred Stochastic Volatility

Helmut Lutkepohl<sup>a</sup>, Fei Shang<sup>b</sup>, Luis Uzeda<sup>c,\*</sup>, Tomasz Woźniak<sup>d,\*\*</sup>

<sup>a</sup>Freie Universität Berlin & DIW Berlin, Freie Universität Berlin, Boltzmannstr. 20, 14195 Berlin, Germany

<sup>b</sup>Guangdong University of Foreign Studies, Xiaoguowei, Panyu District, Guangzhou 510006, China

<sup>c</sup>Bank of Canada, 234 Wellington St. W, Ottawa, ON K1A 0G9

<sup>d</sup>University of Melbourne, 111 Barry St., 3053 Carlton, VIC, Australia

---

---

## A. Priors

### A.1. Multivariate prior for stochastic volatility

Our prior assumptions also imply the joint distributions for the sequences of latent variables related to the volatility processes. In what follows, we first define two new multivariate distributions and use them subsequently to state the joint distributions of conditional variances and their logarithms (see [Tsonas, 2017](#); [Izzeldin, Tsonas, and Michaelides, 2019](#), on the role of joint specification in posterior inference).

**Definition 1. (Multivariate normal product distribution)** Let  $x$  be a scalar zero-mean normally distributed random variable with variance  $\sigma^2$  that is independent of a  $T \times 1$  zero-mean normal vector  $\mathbf{Y}$  with covariance  $\Sigma$ . Then, a random vector  $\mathbf{Z} = x\mathbf{Y}$  follows a  $T$ -variate normal product distribution with zero mean and covariance equal to  $\sigma^2\Sigma$ , denoted by  $\mathbf{Z} \sim \mathcal{NP}_T(\sigma^2\Sigma)$ , with density:

$$2^{-\frac{T-1}{2}} \pi^{-\frac{T+1}{2}} \det(\Sigma)^{-\frac{1}{2}} \left( \frac{1}{\sigma^2} \mathbf{Z}' \Sigma^{-1} \mathbf{Z} \right)^{-\frac{T-1}{4}} K_{-\frac{T-1}{2}} \left( \sqrt{\frac{1}{\sigma^2} \mathbf{Z}' \Sigma^{-1} \mathbf{Z}} \right). \quad (\text{A.1})$$

□

---

\*The views expressed in this paper are those of the authors and do not necessarily reflect the position of the Bank of Canada.

\*\*Corresponding author. Email address: [tomasz.wozniak@unimelb.edu.au](mailto:tomasz.wozniak@unimelb.edu.au).

**Definition 2. (Multivariate log normal product distribution)** Let a  $T \times 1$  random vector  $\mathbf{Z}$  follow a multivariate normal product distribution:  $\mathbf{Z} \sim \mathcal{NP}_T(\sigma^2 \boldsymbol{\Sigma})$ . Then a  $T \times 1$  random vector  $\mathbf{Q} = \exp(\mathbf{Z})$  obtained by applying the exponent to each of the elements of  $\mathbf{Z}$  follows the multivariate log normal product distribution, denoted by  $\mathbf{Q} \sim \log \mathcal{NP}_T(\sigma^2 \boldsymbol{\Sigma})$ , with density:

$$2^{-\frac{T-1}{2}} \pi^{-\frac{T+1}{2}} \det(\boldsymbol{\Sigma})^{-\frac{1}{2}} \times \det(\text{diag}(\mathbf{Q}))^{-1} \left( \frac{1}{\sigma^2} \log(\mathbf{Q})' \boldsymbol{\Sigma}^{-1} \log(\mathbf{Q}) \right)^{-\frac{T-1}{4}} K_{-\frac{T-1}{2}} \left( \sqrt{\frac{1}{\sigma^2} \log(\mathbf{Q})' \boldsymbol{\Sigma}^{-1} \log(\mathbf{Q})} \right). \quad (\text{A.2})$$

□

Note that the univariate (log-)normal product distributions are special cases of their multivariate versions for  $T = 1$ . The multivariate distributions are useful to state the following joint distributions for the sequences of volatilities:

**Proposition 1. (Joint distributions of conditional volatilities)**

Given the prior specification from Equations (2.7)–(2.9) and (3.1)–(3.5), the joint priors for the  $T \times 1$  vectors containing the latent process  $\mathbf{h}_n$ , log-conditional variances  $\log \sigma_n^2 = \omega_n \mathbf{h}_n$ , and conditional variances  $\sigma_n^2 = \exp(\omega_n \mathbf{h}_n)$  are given by the following  $T$ -variate normal, normal product, and log normal product distributions:

(a)  $\mathbf{h}_n \mid \rho_n \sim \mathcal{N}_T \left( \mathbf{0}_{T \times 1}, \left( \mathbf{H}'_{\rho_n} \mathbf{H}_{\rho_n} \right)^{-1} \right),$

(b)  $\log \sigma_n^2 \mid \rho_n, \sigma_{\omega_n}^2 \sim \mathcal{NP}_T \left( \sigma_{\omega_n}^2 \left( \mathbf{H}'_{\rho_n} \mathbf{H}_{\rho_n} \right)^{-1} \right),$

(c)  $\sigma_n^2 \mid \rho_n, \sigma_{\omega_n}^2 \sim \log \mathcal{NP}_T \left( \sigma_{\omega_n}^2 \left( \mathbf{H}'_{\rho_n} \mathbf{H}_{\rho_n} \right)^{-1} \right),$

□

where  $\mathbf{h}_n = (h_{n,1} \ \dots \ h_{n,T})'$  is a  $T \times 1$  vector and  $\mathbf{H}_{\rho_n}$  is a  $T \times T$  matrix with ones on the main diagonal, with  $-\rho_n$  on the first subdiagonal, and with zeros elsewhere.

## A.2. Prior distribution for the SVAR parameters

Our objectives for setting the joint prior distribution for the structural matrix  $\mathbf{B}_0$  and the autoregressive slope parameters collected in the matrix  $\mathbf{A} = \begin{bmatrix} \mathbf{A}_1 & \dots & \mathbf{A}_p & \mathbf{A}_d \end{bmatrix}$  are that (i) it is conditionally conjugate, and thus, facilitates the derivation of an efficient Gibbs sampler for the estimation of the parameters, (ii) it is a reference prior that does not distort the shape of the likelihood function due to the local identification of the model as defined by [Rubio-Ramírez, Waggoner, and Zha \(2010\)](#), (iii) it can be interpreted as a Minnesota prior proposed by [Doan, Litterman, and Sims \(1984\)](#), and (iv) it enjoys the flexibility of the hierarchical prior specification thanks to which the essential hyper-parameters responsible for the level of shrinkage are estimated as argued by [Giannone, Lenza, and Primiceri \(2015\)](#).

All these objectives are met when the prior for the structural matrix is set to the generalized-normal distribution proposed by [Waggoner and Zha \(2003\)](#) and multivariate normal for the autoregressive parameters. Let  $\mathbf{B}_{0,n}$  and  $\mathbf{A}_n$  denote the  $n^{\text{th}}$  row of the matrices  $\mathbf{B}_0$  and  $\mathbf{A}$ , respectively. Then the prior distribution for matrix  $\mathbf{B}_0$  is proportional to

$$p(\mathbf{B}_0 \mid \gamma_0) \propto \det(|\mathbf{B}_0|)^{\nu-N} \exp \left\{ -\frac{1}{2} \sum_{n=1}^N \frac{1}{\gamma_{0,n}} \mathbf{B}_{0,n} \mathbf{B}'_{0,n} \right\}. \quad (\text{A.3})$$

The parameters of this distribution are further assumed to be equation invariant. That feature makes this distribution the reference prior, which means that it is invariant to the rotations of the structural system up to permutation and sign change of its rows (see [Woźniak and Droumaguet, 2015](#)). The scale matrix of the distribution in (A.3) is set to  $\gamma_{0,n} \mathbf{I}_N$ , where  $\gamma_{0,n}$  is a hyper-parameter, and the shape parameter is set to  $\nu_0 = N$ , which makes the marginal prior distribution for the rows of  $\mathbf{B}_0$  the  $N$ -variate normal distribution with the zero mean and covariance  $\gamma_{0,n} \mathbf{I}_N$ .

The prior distribution for each row of matrix  $\mathbf{A}$  is multivariate normal, sharing features of the Minnesota prior. Therefore, the prior mean of  $\mathbf{A}$  is equal to  $\underline{\mathbf{A}} = \begin{bmatrix} \mathbf{D} & \mathbf{0}_{N \times (N(p-1)+d)} \end{bmatrix}$ , where  $\mathbf{D}$  is a diagonal matrix with zeros and ones on the diagonal depending on whether

the corresponding variables in  $\mathbf{y}_t$  are stationary or unit-root non-stationary. The matrix  $\mathbf{D}$  is fixed at  $\mathbf{I}_N$  if all variables in  $\mathbf{y}_t$  are unit-root non-stationary or at  $\mathbf{0}_{N \times N}$  if they are stationary. The covariances of the rows of  $\mathbf{A}$  are given by diagonal matrices  $\gamma_{A,n} \underline{\mathbf{\Omega}}$  with scalar hyperparameters  $\gamma_{A,n}$ , and where  $\underline{\mathbf{\Omega}} = \text{diag}(\mathbf{p}^{-1'} \otimes \mathbf{1}'_N \quad 100\mathbf{1}'_d)$ ,  $\mathbf{p}^{-1}$  denotes a vector containing the reciprocal of integer values from 1 to  $p$ . This matrix provides the increasing level of shrinkage with increasing lag order of the autoregressive slope parameters, incorporating the ideas of the Minnesota prior of [Doan et al. \(1984\)](#). Furthermore, the prior variances of the parameters corresponding to the deterministic terms are equal to  $100\gamma_A$ , reflecting a popular view that the shrinkage should be relatively weaker for these parameters.

Extending the prior by [Giannone et al. \(2015\)](#), the levels of shrinkage of the autoregressive and structural matrices follow a 3-level global-local hierarchical prior on the equation-specific shrinkage parameters  $\gamma_{A,n}$  and  $\gamma_{0,n}$ :

$$\gamma_{0,n} \mid \underline{s}_{0,n} \sim \text{IG2}(\underline{s}_{0,n}, \underline{v}_0), \quad \underline{s}_{0,n} \mid \underline{s}_{\gamma_{0,n}} \sim \mathcal{G}(\underline{s}_{\gamma_0}, \underline{v}_{\gamma_0}), \quad \underline{s}_{\gamma_0} \sim \text{IG2}(\underline{s}_{s_0}, \underline{v}_{s_0}), \quad (\text{A.4})$$

$$\gamma_{A,n} \mid \underline{s}_{A,n} \sim \text{IG2}(\underline{s}_{A,n}, \underline{v}_A), \quad \underline{s}_{A,n} \mid \underline{s}_{\gamma_{A,n}} \sim \mathcal{G}(\underline{s}_{\gamma_A}, \underline{v}_{\gamma_A}), \quad \underline{s}_{\gamma_A} \sim \text{IG2}(\underline{s}_{s_A}, \underline{v}_{s_A}). \quad (\text{A.5})$$

We set  $\underline{v}_0$ ,  $\underline{v}_{\gamma_0}$ ,  $\underline{s}_{s_0}$ , and  $\underline{v}_{s_0}$  to values 10, 10, 100, and 1, respectively, to make the marginal prior for the elements of  $\mathbf{B}_0$  quite dispersed, and  $\underline{v}_A$ ,  $\underline{v}_{\gamma_A}$ ,  $\underline{s}_{s_A}$ , and  $\underline{v}_{s_A}$  all equal to 10, which facilitates relatively strong shrinkage for the autoregressive parameters in matrix  $\mathbf{A}$  that gets updated, nevertheless. Providing sufficient flexibility on this 3-level hierarchical prior distribution was essential for a robust shape of the estimated impulse responses.

### A.3. Prior for conditional variances in a centred SV model

Consider a centred SV model from Equations (2.4)–(2.6) with the inverted-gamma 2 prior for the SV conditional variance parameter:

$$\omega_n^2 \mid \sigma_{\omega_n}^2 \sim \text{IG2}(\sigma_{\omega_n}^2, \underline{v}). \quad (\text{A.6})$$

Then,

- (a) the log-volatilities,  $\tilde{h}_{n,t}$ , follow a Student-t marginal prior distribution (see [Bauwens, Lubrano, and Richard, 1999](#)),
- (b) the conditional variances,  $\sigma_{n,t}^2$ , follow a log-Student-t marginal prior distribution (see [Hogg and Klugman, 1983](#)),
- (c) the prior distribution stated in (b) has a pole at point 0, unless  $\underline{\nu}$  goes to infinity (see [Callealta Barroso, García-Pérez, and Prieto-Alaiz, 2020](#), for points (c)–(e)),
- (d) the prior distribution stated in (b) has a second mode—a local maximum—at point  $\exp\left\{-\frac{1}{2}\left[\underline{\nu} + 1 - \sqrt{(\underline{\nu} + 1)^2 - 4\sigma_{\omega_n}^2}\right]\right\}$  iff  $\sigma_{\omega_n}^2 < \frac{(\underline{\nu}+1)^2}{4}$ ,
- (e) the prior distribution stated in (b) has a median at point 1 only if  $\underline{\nu}$  goes to infinity.  $\square$

These properties show that the unrestricted centred SV parameterization can be highly problematic in SVAR applications. With unconstrained  $\omega_n^2$ , it does not ensure even the normalization of the system about value  $\sigma_{n,t}^2 = 1$ . Moreover, with any finite values of the shape hyper-parameter,  $\underline{\nu}$ , the pole at point 0 provides heavy local shrinkage towards a point where the model is singular as it exhibits zero conditional variances of the structural shocks. In this context, our proposal satisfying all the stated objectives leads to reliable posterior estimates and inferences.

## B. The Gibbs sampler for posterior simulation

This section scrutinizes the estimation procedure that belongs to the class of MCMC methods. The assumptions regarding the distribution of residuals and the prior distribution of the parameters of the model result in a convenient and efficient Gibbs sampler that performs excellently even for larger systems of variables.

### B.1. Sampling SVAR parameters

The conjugate prior distribution for matrix  $\mathbf{B}_0$  results in a convenient generalized-normal full conditional posterior distribution that is proportional to

$$p(\mathbf{B}_0 \mid \mathbf{y}, \mathbf{A}, \sigma_1^2, \dots, \sigma_N^2, \gamma_0) \propto \det(|\mathbf{B}_0|)^{\bar{\nu}-N} \exp \left\{ -\frac{1}{2} \sum_{n=1}^N \mathbf{B}_{0,n} \bar{\mathbf{S}}_n^{-1} \mathbf{B}'_{0,n} \right\} \quad (\text{B.1})$$

$$\bar{\mathbf{S}}_n^{-1} = \mathbf{I}_N / \gamma_{0,n} + \sum_{t=1}^T \mathbf{u}_t \mathbf{u}'_t / \sigma_{n,t}^2 \quad (\text{B.2})$$

$$\bar{\nu} = T + \underline{\nu}. \quad (\text{B.3})$$

The random number generator from this distribution follows the algorithm by [Waggoner and Zha \(2003\)](#). Our experience clearly indicates its fast convergence and efficient extraction of the global shape of the posterior distribution, as pointed out by [Woźniak and Droumaguet \(2015\)](#).

In order to sample the autoregressive parameters  $\mathbf{A}$ , we follow the row-by-row algorithm by [Chan, Koop, and Yu \(2024\)](#) that reduces the number of operations to be performed by the computer by orders of magnitude in comparison to sampling all the parameters at once. Each of the rows, denoted by  $\mathbf{A}_n$ , is sampled from a conditional multivariate normal distribution given all other rows and parameters, and data. Denote by  $\mathbf{A}_0^{(n)}$  an  $N \times K$  matrix filled with the elements of matrix  $\mathbf{A}$  and zeros in the  $n^{\text{th}}$  row, and an  $(Np + d)$ -vector  $\mathbf{x}_t = \begin{bmatrix} \mathbf{y}'_{t-1} & \dots & \mathbf{y}'_{t-p} & d'_t \end{bmatrix}'$ . Then the structural-form model can be written as

$$\mathbf{B}_0 (\mathbf{y}_t - \mathbf{A}_0^{(n)} \mathbf{x}_t) = (\mathbf{B}_{0,n} \otimes \mathbf{x}'_t) \mathbf{A}'_n + \mathbf{w}_t. \quad (\text{B.4})$$

Define an  $N$ -vector  $\mathbf{z}_t^{(n)} = \mathbf{B}_0 (\mathbf{y}_t - \mathbf{A}_0^{(n)} \mathbf{x}_t)$  and an  $N \times (NP + d)$  matrix  $\mathbf{W}_t^{(n)} = (\mathbf{B}_{0,n} \otimes \mathbf{x}'_t)$ .

Then, the full conditional posterior distribution for the vector  $\mathbf{A}_n$  is given by

$$\mathbf{A}'_n | \mathbf{y}, \mathbf{A}_0^{(n)}, \mathbf{B}_0, \sigma_1^2, \dots, \sigma_N^2, \gamma_A \sim \mathcal{N}_{Np+d}(\bar{\mathbf{V}}_n \bar{\mathbf{A}}_n, \bar{\mathbf{V}}_n) \quad (\text{B.5})$$

$$\bar{\mathbf{V}}_n^{-1} = \underline{\mathbf{\Omega}}^{-1} / \gamma_{A.n} + \sum_{t=1}^T \mathbf{W}_t^{(n)'} \text{diag}(\sigma_{1,t}^2, \dots, \sigma_{N,t}^2)^{-1} \mathbf{W}_t^{(n)} \quad (\text{B.6})$$

$$\bar{\mathbf{A}}_n = \underline{\mathbf{\Omega}}^{-1} \underline{\mathbf{A}}'_n / \gamma_{A.n} + \sum_{t=1}^T \mathbf{W}_t^{(n)'} \text{diag}(\sigma_{1,t}^2, \dots, \sigma_{N,t}^2)^{-1} \mathbf{z}_t^{(n)}, \quad (\text{B.7})$$

where  $\underline{\mathbf{A}}_n$  is the  $n^{\text{th}}$  row of  $\underline{\mathbf{A}}$ .

The hierarchy of the structural matrix hyper-parameters  $\gamma_{0.n}$ ,  $\underline{s}_{0.n}$  and  $\underline{s}_{\gamma_0}$  is sampled from their respective full conditional posterior distributions:

$$\gamma_{0.n} | \mathbf{B}_{0.n} \sim \text{IG2}(\underline{s}_{0.n} + \mathbf{B}_{0.n} \mathbf{B}'_{0.n}, \underline{v}_0 + N^2) \quad (\text{B.8})$$

$$\underline{s}_{0.n} | \gamma_B, \underline{s}_{\gamma_0} \sim \mathcal{G}((\underline{s}_{\gamma_0}^{-1} + (2\gamma_{0.n})^{-1})^{-1}, \underline{v}_{\gamma_0} + 0.5\underline{v}_0) \quad (\text{B.9})$$

$$\underline{s}_{\gamma_0} | \underline{s}_0 \sim \text{IG2}\left(\underline{s}_{s_0} + 2 \sum_{n=1}^N \underline{s}_{0.n} \underline{v}_{s_0} + 2N\underline{v}_{\gamma_0}\right), \quad (\text{B.10})$$

whereas the hierarchy of the autoregressive hyper-parameters  $\gamma_{A.n}$ ,  $\underline{s}_{A.n}$  and  $\underline{s}_{\gamma_A}$  is sampled from

$$\gamma_{A.n} | \mathbf{A}_n, \underline{s}_{A.n} \sim \text{IG2}(\underline{s}_{A.n} + (\mathbf{A}_n - \underline{\mathbf{A}}_n) \underline{\mathbf{\Omega}}^{-1} (\mathbf{A}_n - \underline{\mathbf{A}}_n)', \underline{v}_A + Np + d) \quad (\text{B.11})$$

$$\underline{s}_{A.n} | \gamma_{A.n}, \underline{s}_{\gamma_A} \sim \mathcal{G}((\underline{s}_{\gamma_A}^{-1} + (2\gamma_{A.n})^{-1})^{-1}, \underline{v}_{\gamma_A} + 0.5\underline{v}_A) \quad (\text{B.12})$$

$$\underline{s}_{\gamma_A} | \underline{s}_A \sim \text{IG2}\left(\underline{s}_{s_A} + 2 \sum_{n=1}^N \underline{s}_{A.n} \underline{v}_{s_A} + 2N\underline{v}_{\gamma_A}\right). \quad (\text{B.13})$$

## B.2. Sampling stochastic volatility states and related parameters

The Gibbs sampler for the parameters of the SV processes results from our prior assumptions and the normality assumption for the structural shocks ( $w_{n,t}$ ). It is facilitated by using the auxiliary mixture sampler proposed by [Omori, Chib, Shephard](#),

and Nakajima (2007). To this end, note that each structural shock can be written as

$$w_{n,t} = \sqrt{\sigma_{n,t}^2} \epsilon_{n,t}, \quad (\text{B.14})$$

$$\epsilon_{n,t} \sim \mathcal{N}(0, 1). \quad (\text{B.15})$$

By squaring and taking the logarithm of both sides of Equation (B.14) and remembering that we define  $\sigma_{n,t}^2 = \exp(\omega_n h_{n,t})$ , we have

$$\tilde{w}_{n,t} = \omega_n h_{n,t} + \tilde{\epsilon}_{n,t}, \quad (\text{B.16})$$

where  $\tilde{w}_{n,t} = \log w_{n,t}^2$  and  $\tilde{\epsilon}_{n,t} = \log \epsilon_{n,t}^2$ . Given the standard normal assumption for  $\epsilon_{n,t}$  in (B.15), the distribution of  $\tilde{\epsilon}_{n,t}$  is  $\log \chi_1^2$ . This non-standard distribution is approximated precisely by a mixture of ten normal distributions defined by Omori et al. (2007). Applying the auxiliary mixture technique makes the linear Equation (B.16) conditionally normal given the mixture component indicators, which greatly simplifies the sampling algorithm. This mixture of normals is specified by  $s_{n,t} = 1, \dots, 10$ —the mixture component indicator for the  $n^{\text{th}}$  equation at time  $t$ , the normal component probability  $\pi_{s_{n,t}}$ , mean  $\mu_{s_{n,t}}$ , and variance  $\sigma_{s_{n,t}}^2$ . The latter three parameters are fixed and given in Omori et al. (2007), while  $s_{n,t}$  augments the parameter space and is estimated. Its prior distribution is multinomial with probabilities  $\pi_{s_{n,t}}$ . Finally, define  $T \times 1$  vectors:  $\mathbf{s}_n = (s_{n,1} \dots s_{n,T})'$  collecting the realizations of  $s_{n,t}$  for all  $t$ ,  $\boldsymbol{\mu}_{\mathbf{s}_n} = (\mu_{s_{n,1}} \dots \mu_{s_{n,T}})'$ , and  $\boldsymbol{\sigma}_{\mathbf{s}_n}^2 = (\sigma_{s_{n,1}}^2 \dots \sigma_{s_{n,T}}^2)'$  collecting the  $n^{\text{th}}$  equation auxiliary mixture means and variances, and  $\tilde{\mathbf{w}}_n = (\tilde{w}_{n,1} \dots \tilde{w}_{n,T})'$ .

Sampling latent volatilities  $\mathbf{h}_n$  proceeds independently for each  $n$  from the following  $T$ -variate normal distribution parameterized following Chan and Jeliazkov (2009) in terms

of its precision matrix  $\bar{\mathbf{V}}_{h_n}$  and location vector  $\bar{\mathbf{h}}_n$  as

$$\mathbf{h}_n \mid \mathbf{y}, \mathbf{s}_n, B_0, B_+, \omega_n, \rho_n \sim \mathcal{N}_T(\bar{\mathbf{V}}_{h_n} \bar{\mathbf{h}}_n, \bar{\mathbf{V}}_{h_n}) \quad (\text{B.17})$$

$$\bar{\mathbf{V}}_{h_n}^{-1} = \omega_n^2 \text{diag}(\sigma_{\mathbf{s}_n}^{-2}) + \mathbf{H}'_{\rho_n} \mathbf{H}_{\rho_n} \quad (\text{B.18})$$

$$\bar{\mathbf{h}}_n = \omega_n \text{diag}(\sigma_{\mathbf{s}_n}^{-2})(\tilde{\mathbf{w}}_n - \boldsymbol{\mu}_{\mathbf{s}_n}). \quad (\text{B.19})$$

The distinguishing feature of the precision matrix is that it is tridiagonal, which greatly improves the speed of generating random numbers from this full conditional posterior distribution if only the appropriate simulation smoother proposed by [McCausland, Miller, and Pelletier \(2011\)](#) is implemented.

The parameters that are essential for the assessment of identification of the SVAR models,  $\omega_n$ , are sampled independently from the following normal distribution:

$$\omega_n \mid \mathbf{y}, \mathbf{s}_n, h_n, \sigma_{\omega_n}^2 \sim \mathcal{N}(\bar{v}_{\omega_n} \bar{\omega}_n, \bar{v}_{\omega_n}) \quad (\text{B.20})$$

$$\bar{v}_{\omega_n}^{-1} = \mathbf{h}'_n \text{diag}(\sigma_{\mathbf{s}_n}^{-2}) \mathbf{h}_n + \sigma_{\omega_n}^{-2} \quad (\text{B.21})$$

$$\bar{\omega}_n = \mathbf{h}'_n \text{diag}(\sigma_{\mathbf{s}_n}^{-2})(\tilde{\mathbf{w}}_n - \boldsymbol{\mu}_{\mathbf{s}_n}). \quad (\text{B.22})$$

Next, proceed to the ancillarity-sufficiency interweaving sampler proposed by [Kastner and Frühwirth-Schnatter \(2014\)](#). They show that sampling directly the parameters of the centred SV model leads to an efficient sampler if data is heteroskedastic, but it leads to substantial inefficiencies if data is homoskedastic. On the other hand, sampling directly parameters of the non-centred SV parameterization leads to efficient sampling for homoskedastic data but not for heteroskedastic series. The solution offering the optimal strategy when the heteroskedasticity is uncertain and to be verified, is to apply an ancillarity-sufficiency interweaving step in the Gibbs sampler. Our implementation proceeds as follows: Having sampled the random vector  $\mathbf{h}_n$  and parameter  $\omega_n$ , compute the parameters of the centred parameterization  $\tilde{h}_{n,t} = \omega_n h_{n,t}$  and

$\sigma_{v_n}^2 = \omega_n^2$ . Then, sample  $\sigma_{v_n}^2$  from the following full conditional posterior distribution:

$$\sigma_{v_n}^2 \mid \mathbf{y}, \tilde{\mathbf{h}}_n, \sigma_{\omega_n}^2 \sim \mathcal{GIG}\left(-\frac{T-1}{2}, \tilde{\mathbf{h}}_n' \mathbf{H}'_{\rho_n} \mathbf{H}_{\rho_n} \tilde{\mathbf{h}}_n, \sigma_{\omega_n}^{-2}\right), \quad (\text{B.23})$$

where  $\tilde{\mathbf{h}}_n = (\tilde{h}_{n.1} \dots \tilde{h}_{n.T})$ . Finally, compute  $\omega_n = \pm \sqrt{\sigma_{v_n}^2}$  and  $h_{n.t} = \frac{1}{\omega_n} \tilde{h}_{n.t}$  and return them as the MCMC draws for these parameters.

The autoregressive parameters of the SV equations are sampled independently from the following truncated normal distribution:

$$\rho_n \mid \mathbf{y}, h_n, \sigma_{\omega_n}^2 \sim \mathcal{N}\left(\left(\sum_{t=0}^{T-1} h_{n,t}^2\right)^{-1} \left(\sum_{t=1}^T h_{n,t} h_{n,t-1}\right), \left(\sum_{t=0}^{T-1} h_{n,t}^2\right)^{-1}\right) \mathcal{I}\left(|\rho_n| < \sqrt{1 - \sigma_{\omega_n}^2}\right). \quad (\text{B.24})$$

This sampler is performed using the algorithm proposed by [Robert \(1995\)](#) and implemented in the **R** package **RcppTN** by [Olmsted \(2017\)](#).

The prior variances of parameter  $\omega_n, \sigma_{\omega_n}^2$ , are *a posteriori* sampled independently from the following generalized inverse Gaussian distribution:

$$\sigma_{\omega_n}^2 \mid \mathbf{y}, \omega_n \sim \mathcal{GIG}\left(\underline{A} - \frac{1}{2}, \omega_n^2, \frac{2}{\underline{S}}\right), \quad (\text{B.25})$$

using the algorithm introduced by [Hörmann and Leydold \(2014\)](#) and implemented in the **R** package **GIGrvg** by [Leydold and Hörmann \(2017\)](#).

Finally, the auxiliary mixture indicators  $s_{n,t}$  are each sampled independently from a multinomial distribution with the probabilities proportional to the product of the prior probabilities  $\pi_{s_{n,t}}$  and the conditional likelihood function.

### B.3. Computational considerations

The computations reproducing our results can be performed using the **R** package **bsvars** by [Woźniak \(2024, 2025\)](#) that contains our data set with observations until 2022. It contains a compiled code implementing the developed Gibbs sampler as well as the computations for the SDDR and other objects in **C++** using the **R** package **Rcpp** by

Eddelbuettel, François, Allaire, Ushey, Kou, Russel, Chambers, and Bates (2011) and Eddelbuettel (2013) for convenient interfacing with **R**, and the package **RcppArmadillo** by Eddelbuettel and Sanderson (2014) for algebraic operations and sampling random matrices. The **C++** source code for some low-level utility functions is taken from the open-source package **stochvol** by Hosszejni and Kastner (2021). The computations for this paper were performed at the Spartan HPC-Cloud Hybrid (see Meade, Lafayette, Sauter, and Tosello, 2017) at the University of Melbourne.

### C. Computing the Savage-Dickey density ratio

The SDDR can be easily computed as long as the densities of the full conditional posterior and the prior distributions are of a known analytical form. In Appendix C, we show that  $\omega_n$  can be independently sampled from the univariate normal full conditional posterior distributions with the mean  $\bar{\omega}_n$  and variance  $\bar{v}_{\omega_n}$  specified in Equations (B.20)–(B.22). Then, the numerator of the SDDR can be computed using a sample of  $S$  draws from the posterior distribution by applying the marginal density ordinate estimator proposed by Gelfand and Smith (1990):

$$\widehat{p}(\omega_n = 0 \mid \mathbf{y}) = \frac{1}{S} \sum_{s=1}^S f_{\mathcal{N}}\left(0; \bar{\omega}_n^{(s)}, \bar{v}_{\omega_n}^{(s)}\right), \quad (\text{C.1})$$

where  $f_{\mathcal{N}}$  denotes the density function of a normal distribution, whereas  $\bar{\omega}_n^{(s)}$  and  $\bar{v}_{\omega_n}^{(s)}$  denote the values of the mean and variance in which the place of the parameters of the model are replaced by their  $s^{\text{th}}$  draws from the posterior.

### D. Checking alternative ordering rules

One may wonder how much our results depend on the BP-ordering of our draws from the posterior of  $\mathbf{B}_0$ . Therefore, we have repeated our sampling using the estimates obtained by MR to order the rows of the  $\mathbf{B}_0$  drawings (see Appendix F). The results of the SDDRs based on the MR-ordering are presented in Table D.1(a). They paint a similar picture as

the results in Table 3. The evidence for shocks identified through heteroskedasticity is overwhelming in the 2023-sample. It is weaker for the 2006-sample and hardly existent in the MR-sample.

Table D.1: Verification of identification through heteroskedasticity of the structural shocks (based on alternative orderings)

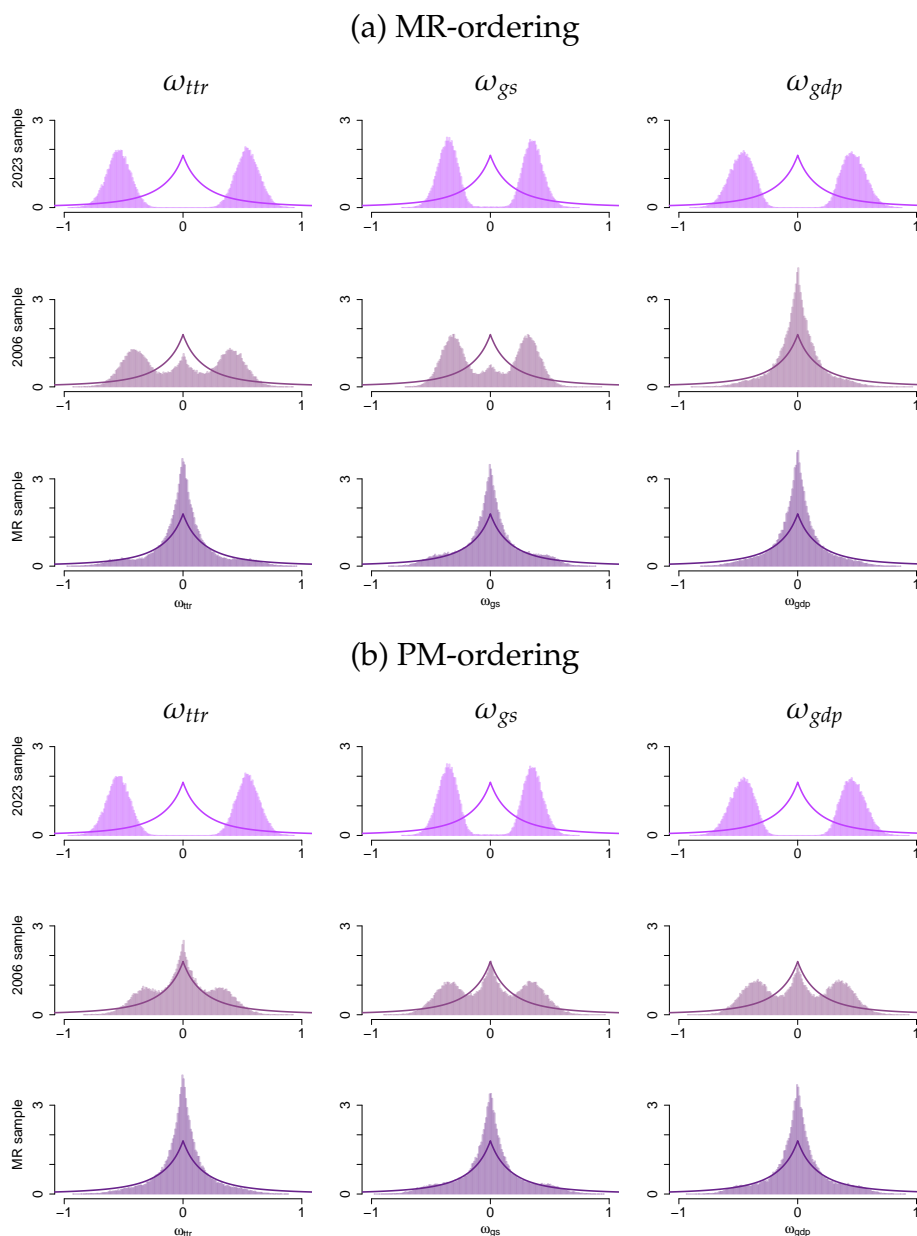
	2023-sample		2006-sample		MR-sample	
(a) MR-ordering						
$w_t^{ttr}$	<b>-21.38</b>	[4.97]	-0.92	[0.14]	0.32	[0.05]
$w_t^{gs}$	<b>-4.62</b>	[0.79]	-1.27	[0.13]	0.24	[0.04]
$w_t^{gdp}$	<b>-32.46</b>	[8.16]	0.38	[0.04]	0.38	[0.03]
(a) PM-ordering						
$w_t^{ttr}$	<b>-21.38</b>	[4.7]	-1.47	[0.2]	0.27	[0.05]
$w_t^{gs}$	<b>-4.62</b>	[0.79]	-1.31	[0.14]	0.52	[0.03]
$w_t^{gdp}$	<b>-63.39</b>	[6.43]	0.35	[0.03]	-0.04	[0.07]

Note: The table reports the log of the Bayes factors estimated via the log of SDDRs together with numerical standard errors provided in brackets.

In Figure D.1(a) we show the marginal prior and posterior densities of the  $\omega_1$  parameter. The picture is very similar to that in Figure 4. In other words, the posterior in the 2023-sample has considerable mass away from the origin and is bi-modal and, hence, strongly supports identified shocks, while the situation is much less clear for the 2006-sample and for the MR-sample, where identification is clearly not supported because the prior and posterior densities are both centred at zero and have considerable density mass in the neighbourhood of zero.

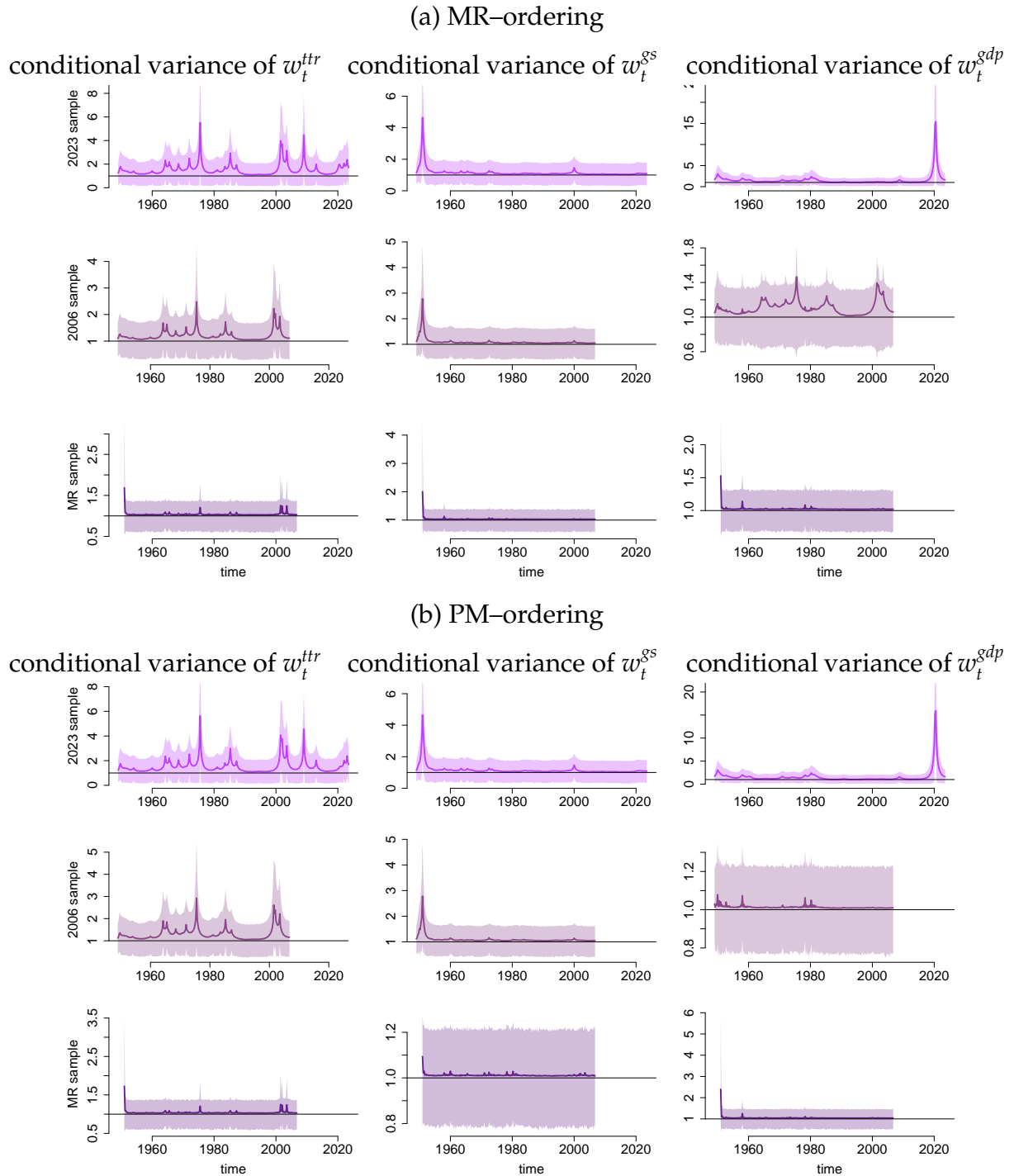
Finally, we show the conditional variances based on the MR-ordering in Figure D.2(a). Comparing that figure to Figure 5, it can be seen that the conditional variances are again very similar to those in the latter figure. Thus, the choice of  $\mathbf{B}_0$  for normalizing the posterior draws is of limited importance. At least, if there is sufficient conditional heteroskedasticity to ensure identification of the shocks, whether we use the BP- or the MR-ordering for the  $\mathbf{B}_0$  drawings is not important.

Figure D.1: Marginal prior (solid line) and posterior (histograms) densities of  $\omega_1$  across samples (based on alternative orderings). The note to Figure 4 applies.



We emphasize, however, that some kind of normalization of the  $\mathbf{B}_0$  drawings is necessary even if the shocks are all well-identified because the structure of the model is invariant to changing the order and sign of the shocks. As long as the normalization ensures a unique ordering and sign of the shocks, it should have little impact on the

Figure D.2: Conditional variance of structural shocks in the three samples (based on alternative orderings). The note to Figure 5 applies.



samples from the posterior distributions if the shocks are well-identified. Therefore, given that for the 2023-sample, we can expect to identify all three shocks through heteroskedasticity, we have also used a target matrix  $\mathbf{B}_0$  for this sample that is not based on a set of estimates from some alternative identification scheme. Instead, we have used a selected posterior mode as the benchmark  $\mathbf{B}_0$  matrix and call it the PM-ordering (see Appendix F for details).

In this case, it is not clear a priori that the ordering of the shocks will be the same as for the BP- and MR-orderings. As the shocks are distinguished by their conditional variances, we consider the conditional variances and order them such that they look similar to those based on the BP- and MR-orderings. In this case, the three distinct variance patterns allow for easily matching them with the shocks from the BP- and MR-orderings so we can easily label the shocks correspondingly. We present the resulting conditional variances in Figure D.2(b).

We have also computed SDDRs and the conditional variances of the three shocks, using the PM-ordering of the  $\mathbf{B}_0$  drawings from the posterior. The results are shown in Table D.1(b). They strongly support that all three shocks are identified through heteroskedasticity in the 2023-sample. In fact, the SDDR values in Table D.1(b) are identical to the corresponding values for the 2023-sample in Table 3. Additionally, the robustness of heteroskedasticity and identification verification to various ordering rules is confirmed by the plots of marginal posterior and prior distributions of  $\omega_n$  for the PM-ordering in Figure D.1 (b), closely resembling other reported figures of this parameter. Thus, as long as some fixed ordering is used to normalize the drawings from the posterior of  $\mathbf{B}_0$ , it does not affect the posterior of the conditional variances and, hence, the identification of the shocks.

## E. Row sign and order normalization

Heteroskedastic SVARs are identified up to the signs and orders of the rows of the structural matrix. Their practical application to the analysis of the sign and order dependent quantities requires transformation of the posterior sample so that it seems

drawn from the posterior region corresponding to the selected row signs and order. We follow the normalization practice by [Lewis \(2021\)](#) and choose the changes of row signs and order of the structural matrix that minimize a distance from the particular posterior draw to the benchmark structural matrix, denoted by  $\widehat{\mathbf{B}}_0$ . Let an  $N \times N$  diagonal scaling matrix  $\mathbf{D}$  with 1 or  $-1$  on the main diagonal and an  $N \times N$  permutation matrix  $\mathbf{P}$  represent the possible row sign and order transformation of  $\mathbf{B}_0^{(s)}$ , denoted by  $\mathbf{PDB}_0^{(s)}$ . We choose those  $\mathbf{D}$  and  $\mathbf{P}$  that minimize the likelihood-based distance proposed by [Jarociński \(2024\)](#):  $\{\text{vec}[(\mathbf{PDB}_0^{(s)} - \widehat{\mathbf{B}}_0)']\}' \widehat{\mathbf{\Omega}}^{-1} \{\text{vec}[(\mathbf{PDB}_0^{(s)} - \widehat{\mathbf{B}}_0)']\}$ , where  $\widehat{\mathbf{\Omega}}$  is the covariance matrix of the asymptotic distribution of the maximum likelihood estimator evaluated at  $\widehat{\mathbf{B}}_0$ . Having chosen the row signs and order, the appropriately transformed draw of the structural matrix is returned and the equation ordering of the SV parameters and latent variables is adjusted accordingly.

Following [Lewis \(2021\)](#), we construct the benchmark  $\widehat{\mathbf{B}}_0$  such that it matches the matrix product on the left-hand side of the equation

$$\begin{bmatrix} \sigma_{ttr} & 0 & 0 \\ 0 & \sigma_{gs} & 0 \\ 0 & 0 & \sigma_{gdp} \end{bmatrix}^{-1} \begin{bmatrix} 1 & \theta_{gs} & 0 \\ \gamma_{ttr} & 1 & 0 \\ 0 & 0 & 1 \end{bmatrix}^{-1} \begin{bmatrix} 1 & 0 & -\theta_{gdp} \\ 0 & 1 & -\gamma_{gdp} \\ -\zeta_{ttr} & -\zeta_{gs} & 1 \end{bmatrix} \begin{bmatrix} u_t^{ttr} \\ u_t^{gs} \\ u_t^{gdp} \end{bmatrix} = \begin{bmatrix} w_t^{ttr} \\ w_t^{gs} \\ w_t^{gdp} \end{bmatrix} \quad (\text{E.1})$$

with the parameter values from the appropriate columns of Table 1 in [Mertens and Ravn \(2014\)](#).

The PM-ordering is chosen by drawing first from the posterior of  $\mathbf{B}_0$  without paying attention to row ordering and sign. Such a sample from the posterior has modes corresponding to the various possible combinations of row signs and orderings. We pick one of the modes and use it for fixing the row signs and orderings in the posterior sample by choosing the row signs and orderings such that Jarociński's likelihood distance is minimized.

## F. Volatility plots under the centred specification for stochastic volatility

For the sake of comparison, we report the conditional variance plots for the SVAR model with an alternative specification for the SV process. We estimated models for all considered data with our priors for matrices  $\mathbf{B}_0$  and  $\mathbf{A}$ , but with the centred SV model by [Chan et al. \(2024\)](#) that is specified similarly to that used by [Cogley and Sargent \(2005\)](#). The model features SV Equations (2.4)–(2.6) together with the prior distributions set following [Chan et al. \(2024\)](#) as

$$\omega_n^2 \sim \text{IG2}(1, 3) \quad \text{and} \quad \rho_n \sim \mathcal{U}(-1, 1). \quad (\text{F.1})$$

Figure F.3: Conditional variance of structural shocks in the three samples for a model with the centred SV specification. The note to Figure 5 applies.

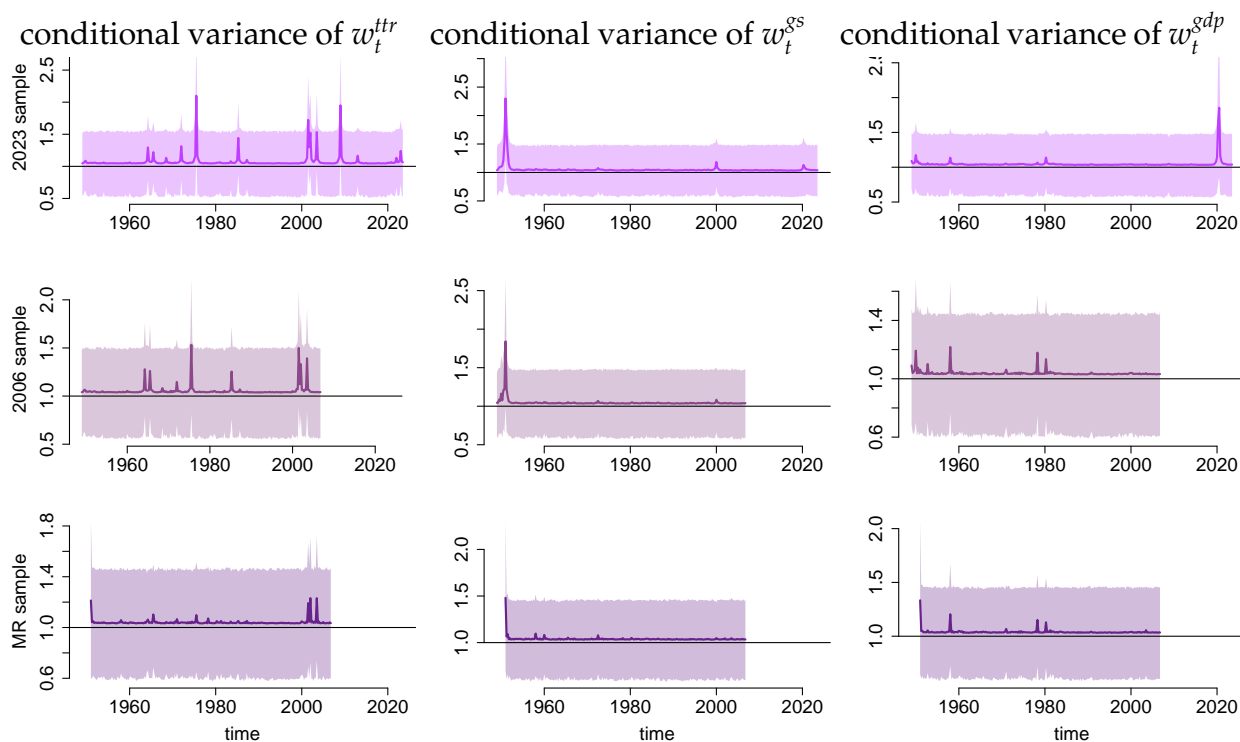


Figure F.3 reports the conditional variances. They have similar shapes as those reported in Figure 5 for our non-centred parameterization of the SV model. In particular,

the periods in which the conditional variances are significantly greater than 1 overlap to a large extent with those for our model for the 2023-sample. Nevertheless, the periods of high volatility are estimated to be more modest than for our model as the variance values in these periods are much lower here. We attribute this phenomenon to the thinner right tail of the prior entertained by the centred parameterization. Note that a more flexible hierarchical prior structure, for instance, estimating the scale of the inverse gamma prior in (F.1) instead of setting it to one, could give this specification greater flexibility.

### G. Supplementary Monte Carlo results on estimation efficiency

We report the results for individual parameters of the top-left-hand-side  $3 \times 3$  block of the estimated matrix in Table G.2 that indicate that estimation efficiency gains are shared by most of the parameters for each DGP.

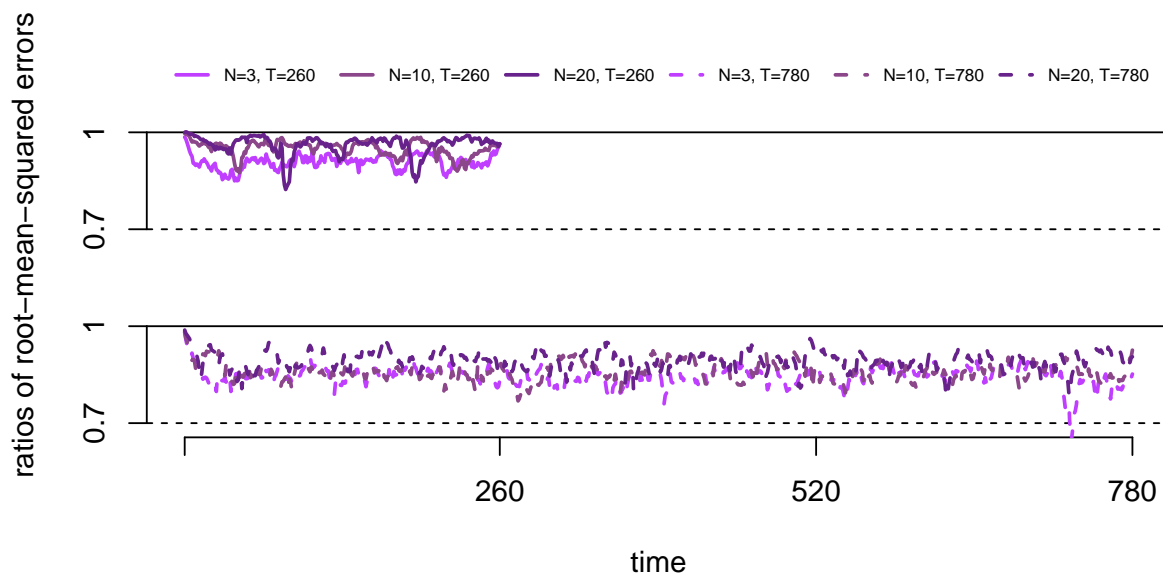
Table G.2: Structural matrix estimation efficiency comparison of models with non-centred and centred SV processes measured by root-mean-squared error of the non-centred SV over the centred SV.

$N$	$T$	$\mathbf{B}_{11}$	$\mathbf{B}_{21}$	$\mathbf{B}_{31}$	$\mathbf{B}_{12}$	$\mathbf{B}_{22}$	$\mathbf{B}_{32}$	$\mathbf{B}_{13}$	$\mathbf{B}_{23}$	$\mathbf{B}_{33}$
3	260	0.85	0.93	1.02	0.99	0.86	0.91	0.86	0.84	0.92
	780	0.71	0.84	0.64	0.90	0.65	0.89	0.76	0.73	0.77
10	260	0.94	1.10	1.05	0.96	0.96	1.19	0.89	1.01	0.92
	780	0.68	1.13	0.73	1.31	0.66	1.26	0.69	1.19	0.68
20	260	0.93	1.18	1.03	1.00	0.97	1.03	0.90	1.10	0.94
	780	0.82	1.60	0.87	0.96	0.80	1.90	0.72	1.45	0.77

Note: The table reports the ratios of the root-mean-squared error for the elements of the structural matrix. We report root-mean-squared errors for the parameters from the top-left-hand-side  $3 \times 3$  block of the  $\mathbf{B}$  matrix in all the systems with  $N = 3, 10,$  and  $20$  variables. The values of ratios smaller than 1 indicate that the parameters in our SVAR model with non-centred SV are estimated more precisely than those with centred SV.

The additional results reported in Figure G.4 show that the estimation efficiency gains of the conditional standard deviations apply to practically every period in the simulated data.

Figure G.4: Comparison of conditional standard deviation estimation efficiency of models with non-centred and centred SV processes measured by period-specific root-mean-squared error.



Note: The figure plots the period-specific ratios of the root-mean-squared errors for the conditional standard deviations,  $\sigma_{n,t}$  for the first three equations of the estimated systems. Systems with 3, 10, and 20 equations are compared, and with sample length of 260 and 780 periods. The values of ratios less than 1 indicate that standard deviations in our SVAR model with non-centred SV are estimated more precisely.

## H. Supplementary Monte Carlo results on rejection rates for other heteroskedasticity-based identification tests

In this section, we report the rejection rates of other procedures that verify identification through heteroskedasticity and consider different hypotheses. Consequently, they are not directly comparable to the results for our procedure reported in Section 5.

The first method is also a Bayesian method and was proposed by [Lütkepohl and Woźniak \(2020\)](#). It investigates identification in the context of an MSH model by checking whether the shock variances in different volatility regimes are sufficiently different for identification through heteroskedasticity. It does so by considering ratios of variances. Table [H.3](#) reports the rejection rates for the  $l$ -value approach for the hypothesis that the variances of the structural shocks are not proportional in a homogeneous two-regime Markov-switching heteroskedasticity model represented by the restriction involving the

Table H.3: Simulation results: Rejection rates for proportional variance changes in a Markov-Switching heteroskedasticity model using the procedure in [Lütkepohl and Woźniak \(2020\)](#)

$T$	homoskedastic shocks in each DGP	DGPs		
		SV	GARCH	MSH
<i>l</i> -value approach				
260	shocks 1 & 2	1.00	1.00	1.00
	shock 1	1.00	1.00	0.99
	shock 2	0.98	0.99	1.00
	none	0.80	0.94	0.51
780	shocks 1 & 2	1.00	1.00	1.00
	shock 1	0.99	1.00	0.97
	shock 2	0.92	0.94	0.99
	none	0.46	0.82	0.51

Note: The table reports rejection rates for the hypothesis of proportional changes in conditional variances  $\mathcal{H}_0 : \sigma_{1,s_t=2}^2 / \sigma_{2,s_t=2}^2 = 1$  investigated using *ln SDDR* by [Lütkepohl and Woźniak \(2020\)](#). The rates are calculated based on 100 realizations of DGPs each with the following characteristics: sample sizes:  $T \in \{260, 780\}$ ; Volatility processes: SV, GARCH, MSH; homoskedastic shock arrangements: shocks 1 & 2, shock 1, shock 2, none. For a homoskedastic shock the variance is set to  $\sigma_n^2 = 1$ .

ration of conditional variances from the second regime  $\sigma_{1,s_t=2}^2 / \sigma_{2,s_t=2}^2 = 1$  and investigated using the Bayes factor (see [Lütkepohl and Woźniak \(2020\)](#) for details). This restriction is sufficient because the conditional variances in the first regime are equal to one.

The procedure performs very well when one shock is hetero- and the other homoskedastic. Its performance significantly weakens when both shocks are heteroskedastic, especially for a heterogeneous Markov process. The Bayes factor performs badly when all shocks are homoskedastic. This is attributed to the fact that [Lütkepohl and Woźniak \(2020\)](#) assume a stationary Markov process requiring non-zero occurrences of each regime. Given this assumption, in homoskedastic data, the second regime picks up a few outlying observations with the regime-specific variances much higher than in the first regime. This leads to the rejection of the hypothesis. Note that [Lütkepohl and Woźniak \(2020\)](#) recommend verifying heteroskedasticity first, for which they provide another Bayesian procedure. Finally, due to this behaviour of the

procedure for homoskedastic data, we were not able to calibrate the critical value for the  $q$ -value approach.

Table H.4 reports the rejection rates for the frequentist tests by [Lanne and Saikkonen \(2007\)](#) and [Lütkepohl and Milunovich \(2016\)](#) used by [Bertsche and Braun \(2022\)](#) and that proposed by [Lewis \(2021\)](#). Not all of these values are comparable with those reported in Table 2 due to different hypotheses verified and the lack of critical values for Bayesian procedures. However, due to our design of the simulation consisting of using the same generated data sets, the rejection rates in the Bayesian  $q$ -value approach and the size-adjusted power simulations are directly comparable across the Panel Bs of Tables 2 and H.4.

[Lanne and Saikkonen \(2007\)](#) proposed two alternative versions of an LM-type test based on Portmanteau test statistics to determine the heteroskedasticity rank defined as the number of independent univariate GARCH processes in the system. [Lütkepohl and Milunovich \(2016\)](#) proposed another LM test for the same set of null hypotheses for a differently specified structural model. We test the null hypothesis that the heteroskedasticity rank is equal to one, which implies identification of the structural shocks for our DGPs. The test proposed by [Lewis \(2021\)](#) verifies the rank order of a specifically constructed matrix involving conditional variances. In order to investigate the hypothesis representing an identified system in our bivariate DGPs, we test the null hypothesis of the rank order being equal to one, which again implies identification of the shocks.

The results indicate that the test by [Lewis \(2021\)](#) and the  $Q_1$  test by [Lanne and Saikkonen \(2007\)](#) exhibit excellent size properties as their empirical sizes nearly perfectly match the nominal size of the tests based on critical values for a 5% level test. The  $Q_1$  test by [Lanne and Saikkonen \(2007\)](#) is consistently undersized, and the test by [Lanne and Saikkonen \(2007\)](#) is consistently oversized in all our samples (see the first row in Panel A of Table H.4). As the test is oversized, its empirical power is somewhat inflated and it is not surprising that its empirical power exceeds that of the [Lewis \(2021\)](#) test. However, even if a small sample correction of the tests is performed as in the size-adjusted power

simulation approach in Panel B of Table H.4, the power of the  $Q_2$  test by [Lanne and Saikkonen \(2007\)](#) is superior in many cases. Exceptions are some DGPs based on MSH processes.

The overall conclusion of our simulations is that none of the procedures works perfectly and is superior for all the scenarios considered in our simulations.

## References

- Bauwens, L., M. Lubrano, and J. Richard (1999). *Bayesian Inference in Dynamic Econometric Models*. Oxford University Press.
- Bertsche, D. and R. Braun (2022). Identification of Structural Vector Autoregressions by Stochastic Volatility. *Journal of Business & Economic Statistics* 40(1), 328–341.
- Callealta Barroso, F. J., C. García-Pérez, and M. Prieto-Alaiz (2020, July). Modelling income distribution using the log Student's  $t$  distribution: New evidence for European Union countries. *Economic Modelling* 89, 512–522.
- Chan, J. and I. Jeliazkov (2009). Efficient Simulation and Integrated Likelihood Estimation in State Space Models. *International Journal of Mathematical Modelling and Numerical Optimisation* 1, 101–120.
- Chan, J. C. C., G. Koop, and X. Yu (2024). Large order-invariant bayesian vars with stochastic volatility. *Journal of Business & Economic Statistics* 42(2), 825–837.
- Cogley, T. and T. J. Sargent (2005). Drifts and Volatilities: Monetary Policies and Outcomes in the Post WWII US. *Review of Economic Dynamics* 8, 262–302.
- Doan, T., R. B. Litterman, and C. A. Sims (1984). Forecasting and Conditional Projection Using Realistic Prior Distributions. *Econometric Reviews* 3(June 2013), 37–41.
- Eddelbuettel, D. (2013). *Seamless R and C++ Integration with Rcpp*. New York, NY: Springer.
- Eddelbuettel, D., R. François, J. Allaire, K. Ushey, Q. Kou, N. Russel, J. Chambers, and D. Bates (2011). Rcpp: Seamless r and c++ integration. *Journal of Statistical Software* 40(8), 1–18.
- Eddelbuettel, D. and C. Sanderson (2014, March). RcppArmadillo: Accelerating R with high-performance C++ linear algebra. *Computational Statistics & Data Analysis* 71, 1054–1063.
- Gelfand, A. E. and A. F. M. Smith (1990, jun). Sampling-Based Approaches to Calculating Marginal Densities. *Journal of the American Statistical Association* 85(410), 398–409.
- Giannone, D., M. Lenza, and G. E. Primiceri (2015). Prior Selection for Vector Autoregressions. *Review of Economics and Statistics* 97(2), 436–451.
- Hogg, R. V. and S. A. Klugman (1983). On the estimation of long tailed skewed distributions with actuarial applications. *Journal of Econometrics* 23(1), 91–102.

- Hörmann, W. and J. Leydold (2014). Generating generalized inverse gaussian random variates. *Statistics and Computing* 24(4), 547–557.
- Hosszejni, D. and G. Kastner (2021). Modeling Univariate and Multivariate Stochastic Volatility in R with **stochvol** and **factorstochvol**. *Journal of Statistical Software* 100(12).
- Izzeldin, M., M. G. Tsionas, and P. G. Michaelides (2019, June). Multivariate Stochastic Volatility with Large and Moderate Shocks. *Journal of the Royal Statistical Society, Series A: Statistics in Society* 182(3), 887–917.
- Jarociński, M. (2024). Estimating the fed’s unconventional policy shocks. *Journal of Monetary Economics*.
- Kastner, G. and S. Frühwirth-Schnatter (2014). Ancillarity-sufficiency interweaving strategy (asis) for boosting mcmc estimation of stochastic volatility models. *Computational Statistics & Data Analysis* 76, 408–423.
- Lanne, M. and P. Saikkonen (2007). A multivariate generalized orthogonal factor garch model. *Journal of Business & Economic Statistics* 25(1), 61–75.
- Lewis, D. J. (2021). Identifying Shocks via Time-Varying Volatility. *The Review of Economic Studies* 88(6), 3086–3124.
- Leydold, J. and W. Hörmann (2017). *GIGrvg: Random Variate Generator for the GIG Distribution*. R package version 0.5.
- Lütkepohl, H. and T. Woźniak (2020). Bayesian inference for structural vector autoregressions identified by Markov-switching heteroskedasticity. *Journal of Economic Dynamics and Control* 113, 103862.
- Lütkepohl, H. and G. Milunovich (2016). Testing for identification in SVAR-GARCH models. *Journal of Economic Dynamics and Control* 73, 241–258.
- McCausland, W. J., S. Miller, and D. Pelletier (2011). Simulation smoothing for state-space models: A computational efficiency analysis. *Computational Statistics & Data Analysis* 55(1), 199–212.
- Meade, B., L. Lafayette, G. Sauter, and D. Tosello (2017). Spartan HPC-Cloud Hybrid: Delivering Performance and Flexibility. *University of Melbourne*.
- Mertens, K. and M. O. Ravn (2014). A reconciliation of SVAR and narrative estimates of tax multipliers. *Journal of Monetary Economics* 68, S1–S19.
- Olmsted, J. (2017). *RcppTN: Rcpp-Based Truncated Normal Distribution RNG and Family*. R package version 0.2-2.
- Omori, Y., S. Chib, N. Shephard, and J. Nakajima (2007). Stochastic Volatility with Leverage: Fast and Efficient Likelihood Inference. *Journal of Econometrics* 140(2), 425–449.
- Robert, C. P. (1995). Simulation of truncated normal variables. *Statistics and Computing* 5(2), 121–125.
- Rubio-Ramírez, J. F., D. F. Waggoner, and T. Zha (2010). Structural Vector Autoregressions: Theory of Identification and Algorithms for Inference. *Review of Economic Studies* 77(2), 665–696.
- Tsionas, M. G. (2017, July). A non-iterative (trivial) method for posterior inference in stochastic volatility

- models. *Statistics & Probability Letters* 126, 83–87.
- Waggoner, D. F. and T. Zha (2003). A Gibbs Sampler for Structural Vector Autoregressions. *Journal of Economic Dynamics & Control* 28(2), 349–366.
- Woźniak, T. (2024). *bsvars: Bayesian Estimation of Structural Vector Autoregressive Models*. R package version 3.2.
- Woźniak, T. (2025). Fast and Efficient Bayesian Analysis of Structural Vector Autoregressions Using the R Package *bsvars*. Working paper, University of Melbourne.
- Woźniak, T. and M. Droumaguet (2015). Assessing Monetary Policy Models: Bayesian Inference for Heteroskedastic Structural VARs. *University of Melbourne Working Papers Series* 2017.

Table H.4: Simulation results: Rejection rates for tests by [Lanne and Saikkonen \(2007\)](#) (LS2007), [Lütkepohl and Milunovich \(2016\)](#) (LM2016), and [Lewis \(2021\)](#). The note to Table 2 applies.

$T$	homoskedastic shocks in each DGP	$Q_1$ by LS2007				$Q_2$ by LS2007				by LM2016				by Lewis (2021)			
		SV	GARCH	MSH	DGPs	SV	GARCH	MSH	DGPs	SV	GARCH	MSH	DGPs	SV	GARCH	MSH	DGPs
Panel A: Based on asymptotic critical values for a 5% level test																	
260	shocks 1 & 2	0.07	0.07	0.07	0.04	0.04	0.04	0.12	0.12	0.12	0.12	0.12	0.04	0.04	0.04	0.04	0.04
	shock 1	0.50	0.24	0.50	0.69	0.80	0.49	0.66	0.81	0.81	0.48	0.30	0.34	0.34	0.33	0.33	0.33
	shock 2	0.69	0.64	0.77	0.60	0.83	0.58	0.63	0.86	0.86	0.49	0.63	0.55	0.55	0.50	0.50	0.50
	none	0.77	0.91	0.84	0.87	0.99	0.81	0.83	0.99	0.99	0.78	0.43	0.72	0.72	0.05	0.05	0.05
780	shocks 1 & 2	0.05	0.05	0.05	0.02	0.02	0.02	0.10	0.10	0.10	0.10	0.10	0.05	0.05	0.05	0.05	0.05
	shock 1	0.87	0.43	0.88	0.92	1.00	0.84	0.93	1.00	1.00	0.81	0.74	0.73	0.65	0.65	0.65	0.65
	shock 2	0.99	0.96	0.97	0.91	1.00	0.93	0.91	1.00	1.00	0.92	0.94	0.95	0.81	0.81	0.81	0.81
	none	0.98	1.00	0.99	0.99	1.00	0.99	0.99	1.00	1.00	0.99	0.77	0.87	0.87	0.02	0.02	0.02
Panel B: Based on the the 5th percentile of the simulated test statistics																	
260	shocks 1 & 2	0.05	0.05	0.05	0.05	0.05	0.05	0.05	0.05	0.05	0.05	0.05	0.05	0.05	0.05	0.05	0.05
	shock 1	0.48	0.24	0.48	0.70	0.81	0.51	0.50	0.68	0.31	0.33	0.37	0.37	0.33	0.33	0.33	0.33
	shock 2	0.69	0.64	0.76	0.60	0.83	0.59	0.51	0.77	0.77	0.30	0.64	0.61	0.53	0.53	0.53	0.53
	none	0.77	0.91	0.84	0.87	0.99	0.81	0.66	0.98	0.98	0.71	0.44	0.74	0.74	0.06	0.06	0.06
780	shocks 1 & 2	0.05	0.05	0.05	0.05	0.05	0.05	0.05	0.05	0.05	0.05	0.05	0.05	0.05	0.05	0.05	0.05
	shock 1	0.87	0.43	0.88	0.93	1.00	0.88	0.92	1.00	1.00	0.74	0.77	0.74	0.69	0.69	0.69	0.69
	shock 2	0.99	0.96	0.97	0.94	1.00	0.93	0.89	1.00	1.00	0.86	0.95	0.95	0.82	0.82	0.82	0.82
	none	0.98	1.00	0.99	0.99	1.00	0.99	0.99	1.00	1.00	0.99	0.78	0.87	0.87	0.02	0.02	0.02